

STATE OF ALASKA
DEPARTMENT OF NATURAL RESOURCES
DIVISION OF GEOLOGICAL AND GEOPHYSICAL SURVEYS

STATE OF ALASKA
Bill Sheffield, *Governor*
Esther C. Wunnicke, *Commissioner, Dept. of Natural Resources*
Ross G. Schaff, *State Geologist*

1984

This report is a preliminary publication of DGGS.
The author is solely responsible for its content and
will appreciate candid comments on the accuracy of
the data as well as suggestions to improve the report.

Report of Investigations 84-13
THE TURNAGAIN HEIGHTS LANDSLIDE:
AN ASSESSMENT USING THE
ELECTRIC-CONE-PENETRATION TEST

By
Randall G. Updike

STATE OF ALASKA
Department of Natural Resources
DIVISION OF GEOLOGICAL & GEOPHYSICAL SURVEYS

According to Alaska Statute 41, the Alaska Division of Geological and Geophysical Surveys is charged with conducting 'geological and geophysical surveys to determine the potential of Alaska lands for production of metals, minerals, fuels, and geothermal resources; the locations and supplies of ground waters and construction materials; the potential geologic hazards to buildings, roads, bridges, and other installations and structures; and shall conduct other surveys and investigations as will advance knowledge of the geology of Alaska.'

In addition, the Division shall collect, evaluate, and publish data on the underground, surface, and coastal waters of the state. It shall also file data from water-well-drilling logs.

DGGS performs numerous functions, all under the direction of the State Geologist---resource investigations (including mineral, petroleum, and water resources), geologic-hazard and geochemical investigations, and information services.

Administrative functions are performed under the direction of the State Geologist, who maintains his office in Anchorage (ph. 276-2653).

This report is for sale by DGGS for \$4. It may be inspected at the following locations: Alaska National Bank of the North Bldg., Geist Rd. and University Ave., Fairbanks; 3601 C St. (10th floor), Anchorage; 400 Willoughby Center (4th floor), Juneau; and the State Office Bldg., Ketchikan.

Mail orders should be addressed to DGGS, 794 University Ave. (Basement), Fairbanks 99701.

CONTENTS

	<u>Page</u>
Introduction.....	1
Scope.....	1
Rationale.....	1
Location of study area.....	1
Geologic history.....	1
Previous investigations.....	3
Testing procedure.....	5
Equipment and method.....	5
Data reduction and interpretation.....	9
Testing results.....	9
Calibration and correlation.....	18
Conclusions.....	31
Acknowledgments.....	33
References cited.....	33
Appendix.....	35

FIGURES

Figure 1. Index map showing location of study area, boreholes, CPT sites, and location of cross-section shown on figure 19.	2
2. Tentative comparison of late Quaternary glacial chronologies in the upper Cook Inlet region with other areas in southern Alaska.....	4
3. CPT laboratory truck with hydraulic jacks extended before initiating sounding	6
4. CPT probe in position to initiate sounding.....	6
5. Close-up of cone assembly with cone and friction sleeve removed to show strain gauges.....	7
6. Cross section of electric-cone assembly.....	8
7. Computer-generated CPT strip charts obtained April 5, 1982, for site EQ-1	10
8. Computer-generated CPT strip charts obtained April 5, 1982, for site EQ-2	11
9. Computer-generated CPT strip charts obtained April 5, 1982, for site EQ-3.....	12
10. Computer-generated CPT strip charts obtained April 7, 1982, for site EQ-4.....	13
11. Computer-generated CPT strip charts obtained April 7, 1982, for site EQ-5.....	14
12. Graph of cone resistance vs. friction ratio for facies F.II and F.III.....	15
13. Graph of cone resistance vs. friction ratio derived from CPT data showing soil-behavior domains for facies of the Bootlegger Cove Formation.....	16
14. Graph showing SPT profile for site EQ-1 as predicted from CPT data.....	19
15. Graph showing SPT profile for site EQ-2 as predicted from CPT data.....	20

16. Graph showing SPT profile for site EQ-3 as predicted from CPT data.....	21
17. Graph showing SPT profile for site EQ-4 as predicted from CPT data.....	22
18. Graph showing SPT profile for site EQ-5 as predicted from CPT data.....	23
19. Geological cross section, Earthquake Park, Anchorage, Alaska.....	26
20. Graph of undrained shear strength vs. depth. Empirical values derived from the CPT for site EQ-3 are compared with laboratory values from boreholes C-133 and C-134..	27
21. Graph of undrained shear strength vs. depth. Empirical values derived from the CPT for sites EQ-4 and EQ-5 (using the equation $S_u = f_s \times 1.10$) are compared with laboratory values from borehole C-140.....	28
22. Graph of undrained shear strength vs. depth. Empirical values derived from the CPT for sites EQ-4 and EQ-5 (using the equations $S_u (q_c - \sigma_v/N)$) are compared with laboratory values from borehole C-140.....	29
23. Graph of undrained shear strength vs. depth. Empirical values derived from the CPT for site EQ-1 are compared with laboratory values from boreholes C-141 and C-142..	30
24. Graph of SPT vs. depth, with field of liquefaction susceptibility.....	32

METRIC CONVERSION FACTORS

To convert feet to meters, multiply by 0.3048. To convert inches to centimeters, multiply by 2.54. To convert miles to kilometers, multiply by 1.61.

THE TURNAGAIN HEIGHTS LANDSLIDE:
AN ASSESSMENT USING THE ELECTRIC-CONE-PENETRATION TEST

By
Randall G. Updike

INTRODUCTION

Scope

The Turnagain Heights landslide was one of the most catastrophic ground failures that resulted from the 1964 Prince William Sound Earthquake. This study assesses the engineering soils responsible for that landslide based on state-of-the-art in-situ testing provided by the electric-cone-penetration-testing system (CPT).

Rationale

The Turnagain Heights area of Anchorage has continued to be an area of residential and light commercial construction since the 1964 earthquake. Engineering soils similar to those that failed in 1964 are being used as the foundation for this construction. Few technical studies of these materials have been conducted since the post-earthquake investigations in 1964-65. Because of economic pressures, the areas immediately adjacent to and within the Turnagain Heights landslide may soon be new construction sites. To benefit future planning and development, the latest geotechnical techniques should be used to assess the present-day in-situ conditions of the soils in question.

Location of Study Area

Five testing sites were chosen in the Municipality of Anchorage Earthquake Park that is located in west Anchorage along a north-facing bluff that borders Knik Arm (fig. 1). The five sites are situated on upland areas south and west of the 1964 landslide, adjacent to West Northern Lights Boulevard (sec. 22, T. 13 N., R. 4 W., Anchorage A-8 NW Quadrangle).

Geologic History

The generalized geology of Anchorage, including the study area, has been mapped by Miller and Dobrovolsky (1959), Karlstrom (1964), and Schmoll and Dobrovolsky (1972). Recently, subsurface geotechnical data was used to make a detailed geologic map of southwest Anchorage (Ulery and Updike, 1983; Updike and Ulery, 1985). These reports show that the Bootlegger Cove Formation, which underlies the study area, was deposited in an ice-marginal glaciolacustrine basin during late Pleistocene time. A glacier located west of Point Woronzof deposited a fan delta that grades from sand and gravel in the west to silt and clay in the Earthquake Park-Turnagain Heights area. Subtle variations in the glaciomarine depositional regime resulted in eight sedimentary facies within the Bootlegger Cove Formation, each defined by a distinct engineering-parametric signature (Updike, 1982). These facies include:

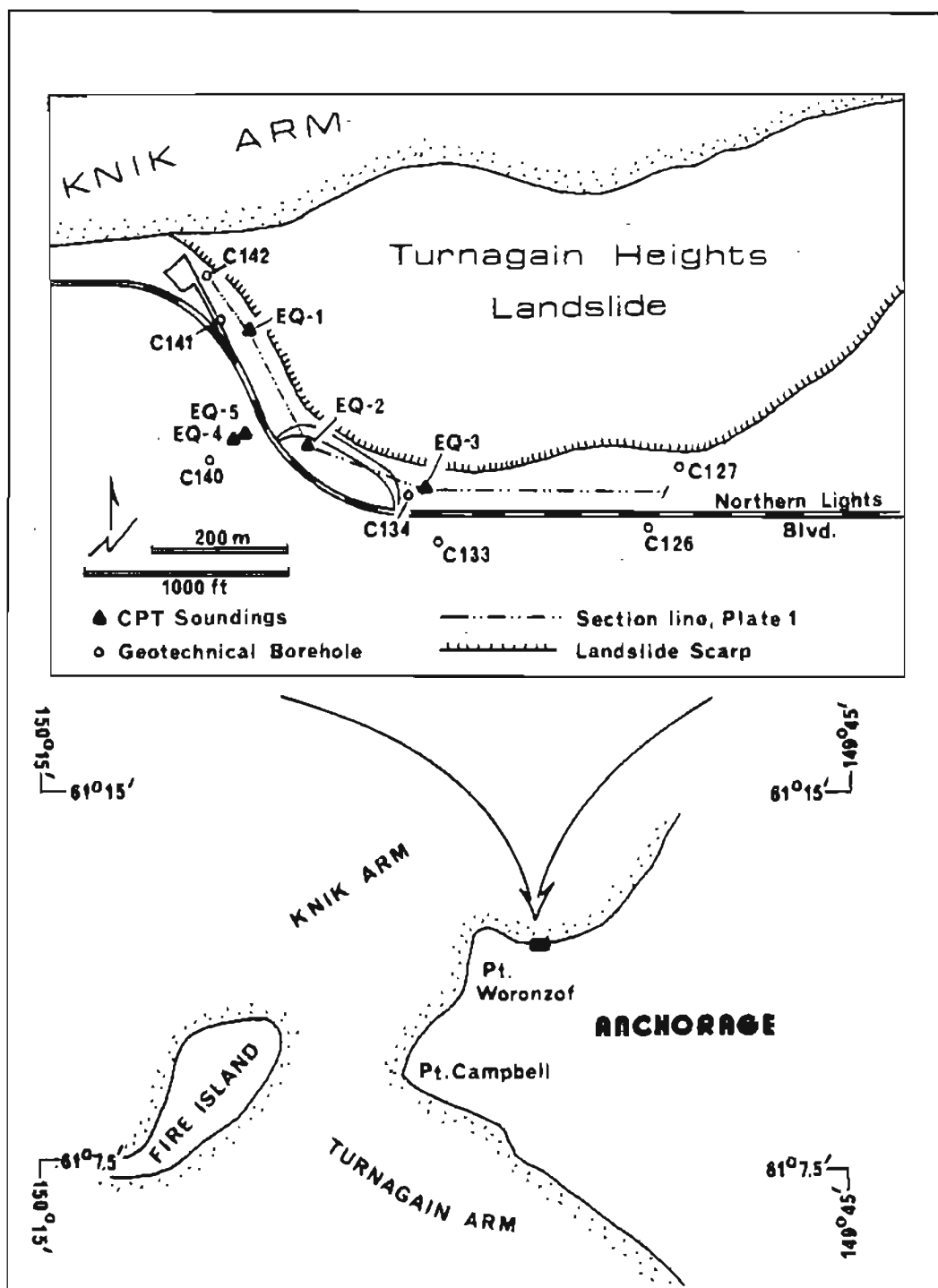


Figure 1. Index map showing location of study area, boreholes, CPT sites, and location of cross section shown on figure 19.

Facies F.I	Clay, with very minor silt and sand
Facies F.II	Silty clay or clayey silt
Facies F.III	Silty clay or clayey silt, sensitive
Facies F.IV	Silty clay or clayey silt, with thin silt and sand lenses
Facies F.V	Silty clay or clayey silt, with random pebbles, cobbles, and boulders
Facies F.VI	Silty fine sand, with silt and clay layers
Facies F.VII	Fine to medium sand, with traces of silt and gravel
Facies F.VIII	Sandy gravel and gravelly sand, with discontinuous layers of silt and fine sand

The Bootlegger Cove Formation was deposited on a sequence of indurated till and glaciofluvial deposits that Reger and Updike (1983) believe is late Pleistocene (Knik Glaciation) in age (fig. 2). A pronounced unconformity exists between these glacial deposits and the overlying Bootlegger Cove Formation, a formation that was probably deposited during late Naptowne time (Reger and Updike, 1983). Within the project area, facies F.I-F.V are capped by very fine to coarse, well-sorted sand beds (facies F.VI and F.VII). These sands represent the waning phase of deposition of the Bootlegger Cove Formation when the source-area ice was stagnant, glacial dams were breached, and the depositional basin was essentially drained. In the Turnagain Heights area and northeast to downtown Anchorage, these sands are overlain by glacial outwash (sand and gravel) deposited during a very late Pleistocene glacial advance from the north that terminated in the Eagle River area. The outwash plain thins to the southwest and eventually disappears just east of the project area. Within the project area, only a thin layer (1 to 5 cm) (0.5 to 2 in.) of tan silt and a surface peat bed overlie the Bootlegger Cove Formation. Facies F.VI-F.VII sands at the top of the formation are typical throughout Anchorage, regardless of the overlying stratigraphy. Consequently, I believe that little erosion of the upper surface of the formation has occurred since deposition in late Pleistocene time (ca. 12,500 yr B.P.).

During Holocene time, the stratigraphic sequence was subjected to isostatic rebound and periodic tectonic uplift (Brown and others, 1977) that, combined with fluctuations in sea level, resulted in the present bluff topography along Knik Arm. The bluffs have gradually retreated because of the effects of tidal erosion and the slope instability of the Bootlegger Cove Formation. Periodic seismic events have enhanced this retreat by causing massive landslides like the one that occurred in Turnagain Heights in 1964.

Previous Investigations

In addition to the geologic mapping described above, the Turnagain Heights landslide was studied intensively after the 1964 earthquake. This landslide, as well as analogous slides elsewhere in Anchorage, prompted

considerable research into the cause and mechanics of such slides. Causes that were proposed in the literature include liquefaction of sands (Shannon and Wilson, 1964; Seed and Wilson, 1967; Seed, 1968, 1976) and failure of sensitive, silty clays (Hansen, 1965; Long and George, 1966; Kerr and Drew, 1965, 1968). The area has become a case-history model for both types of landslide mechanisms. A definitive agreement has not been reached as to which mechanism is primarily responsible for the slides, or whether sands or clays should be of preeminent concern in future potential failures.

The Bootlegger Cove Formation also plays an important role as a confining layer in the ground-water regime of the region. This formation has been the subject of several hydrologic studies (Cederstrom and others, 1964; Trainer and Waller, 1965; Barnwell and others, 1972) and continues to be studied by the U.S. Geological Survey Water Resources Division and the Municipality of Anchorage.

TESTING PROCEDURE

Subsurface soil conditions can be evaluated by drilling, sampling, and laboratory testing, or by in-situ testing. Regardless of the care exercised, the first method has inherent problems with sample disturbance and testing in other than actual conditions. In-situ testing is limited by both the variety of techniques available and by data interpretation based on existing soil-behavior theory. Penetration testing, which is the in-situ approach generally used, is based on the concept that the force or energy required to push or drive a standardized probe into the soil can be translated into a measure of soil strength or bearing capacity. Two principal penetration-test methods are used; the standard-penetration test (SPT) and the cone-penetration test (CPT). The SPT method has been used in Anchorage for many years and remains a standard for local foundation design. Although the CPT method has been used in Europe for several years, it has only recently attained acceptance in the United States geotechnical industry. Although the CPT method has been used for a variety of major projects in the contiguous United States (for example, nuclear power sites, dams, pipeline corridors, and missile sites), this study represents its first usage in Alaska.

Equipment and Method

The cone-penetration test consists of pushing an instrumented, cone-tipped probe into the soil while recording the resistance of the soil to that penetration. The tests were conducted in general accordance with American Society for Testing and Materials specifications (ASTM-D3441-79) using an electric-cone penetrometer. The test equipment consists of a cone assembly, a series of hollow sounding rods, a hydraulic frame to push the cone and rods into the soil, an analog strip-chart recorder, and a truck to transport the test equipment and provide the needed 20-ton thrust-reaction capacity (fig. 3). The cone penetrometer (figs. 4 and 5) consists of a conical tip with a 60° apex angle and a cylindrical friction sleeve above the tip. The cone assembly used on this project has a cross-sectional area of 15 cm² (2.32 in.²), and a sleeve surface area of 200 cm² (31 in.²). Inside the assembly are strain gauges that allow simultaneous measurement of cone and



Figure 3. CPT Laboratory truck with hydraulic jacks extended before initiating sounding (April 5, 1982).

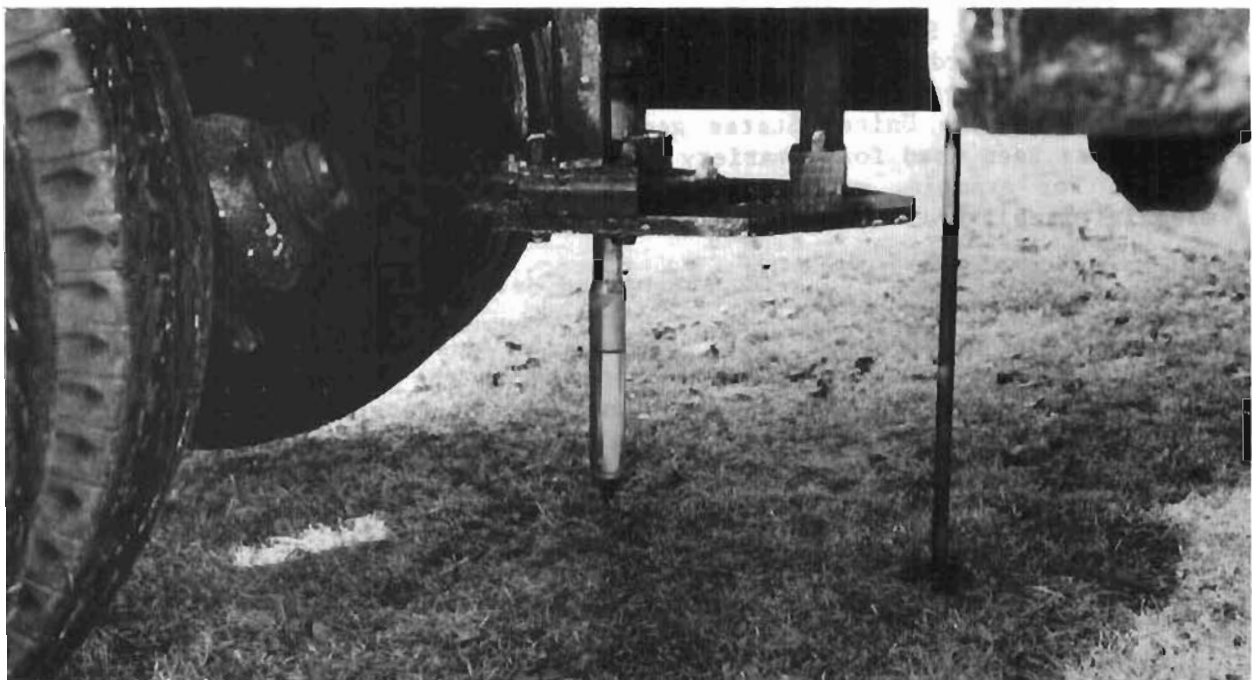


Figure 4. CPT probe in position to initiate sounding. Rod at right is used to calibrate vertical lift of truck during sounding (April 5, 1982).



Figure 5. Close-up of cone assembly with cone and friction sleeve removed to show strain gauges (April 7, 1982).

sleeve resistance during penetration (fig. 6). Continuous electric signals from the strain gauges are transmitted by a cable in the sounding rods to the recorder at the ground surface. In addition, one sounding (EQ-5) was done using the piezo-cone, which simultaneously records pore-water pressure and penetration measurements. The piezo-cone is a standard cone with a

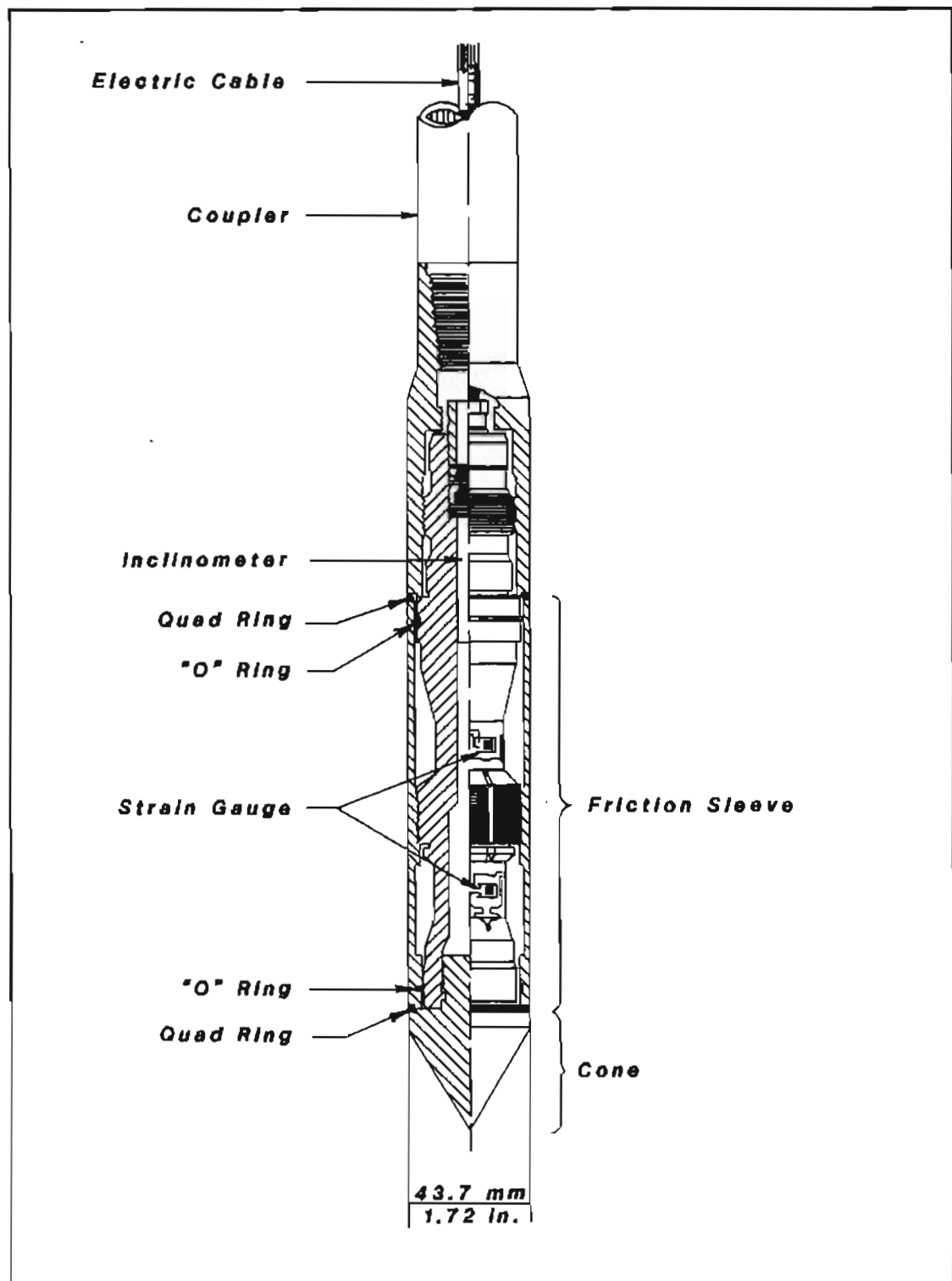


Figure 6. Cross section of electric-cone assembly used in this study (figs. 4 and 5).

pore-pressure transducer and porous element in the conical tip. The piezo-cone records cone-penetrometer data in the same manner as the standard unit.

Data Reduction and Interpretation

Reduction of the CPT data involved digitization of field strip-chart recordings and subsequent computer processing. Processing was done at the data-processing center of Earth Technology Corporation (Ertec), Long Beach, California. In addition to field-data reduction, subroutines that evaluated CPT soil-behavior types, equivalent SPT blow counts, estimated clay shear strengths vs. depth, and cone resistance vs. friction ratio for selected depth intervals were done. Bruce Douglas (Ertec Research Project Engineer), Brenda Meyer (Ertec Civil Engineer), and I interpreted the field data (CPT and adjacent borehole logs) for input into computer programs.

TESTING RESULTS

Five CPT soundings were taken at Earthquake Park on April 5 and 7, 1982. The soundings ranged in total depth from 25 m (76.4 ft) to 40 m (122.1 ft). The resultant strip charts are shown in figures 7 through 11, including the friction resistance (sleeve friction, f_s , in ton/ft²), cone resistance (end bearing, q_c , in ton/ft²), and friction ratio ($R_f = f_s/q_c$). All soundings penetrated the base of the Bootlegger Cove Formation where the Knik diamicton was encountered.

CPT soil-behavior predictions are tabulated in the appendix. The Ertec computer program estimates soil types by tracking the cone-end bearing and average friction ratio at each requested depth. Based on guidelines of a classification chart that evolved from the work of Begemann (1965), Schmertmann (1971), Sanglerat (1972), and Searle (1979), the chart was calibrated to project equipment by Douglas and Olsen (1981). An example of the computer tracking for two soil types at site EQ-2 is shown in figure 12. By comparison of plots of cone resistance (q_c) vs. friction ratio (R_f) (fig. 12) with data from nearby boreholes, site-specific correlations can be made (see Calibration and Correlation). The basic classification chart was modified (as shown in figure 13) and used to tabulate soil-behavior types in the appendix.

The CPT data is averaged over a vertical distance of 11.2 cm (6 in.) to smooth any rapid excursions due to soil-layer interfaces or nonuniformities. However, the material type is calculated at specified depths and, if the tabulation depth occurs at an interface, the data may be inaccurate. Moreover, if the tabulation depth falls in a pocket of material different from the rest of the layer, the data may be misleading. Thus, the continuous penetration-resistance profile is the primary source of profile description, and the soil-type tabulations should be considered supplemental. Further, the tabulated data are defined on the basis of the response of the soil layer to large shear deformations imposed during penetration and not necessarily to predictions of grain-size distribution. However, soil-behavior types shown in figure 13 generally agree with soil types defined in accordance with grain-size-distribution measurements used in the Unified Soil Classification System (Douglas and Olsen, 1981).

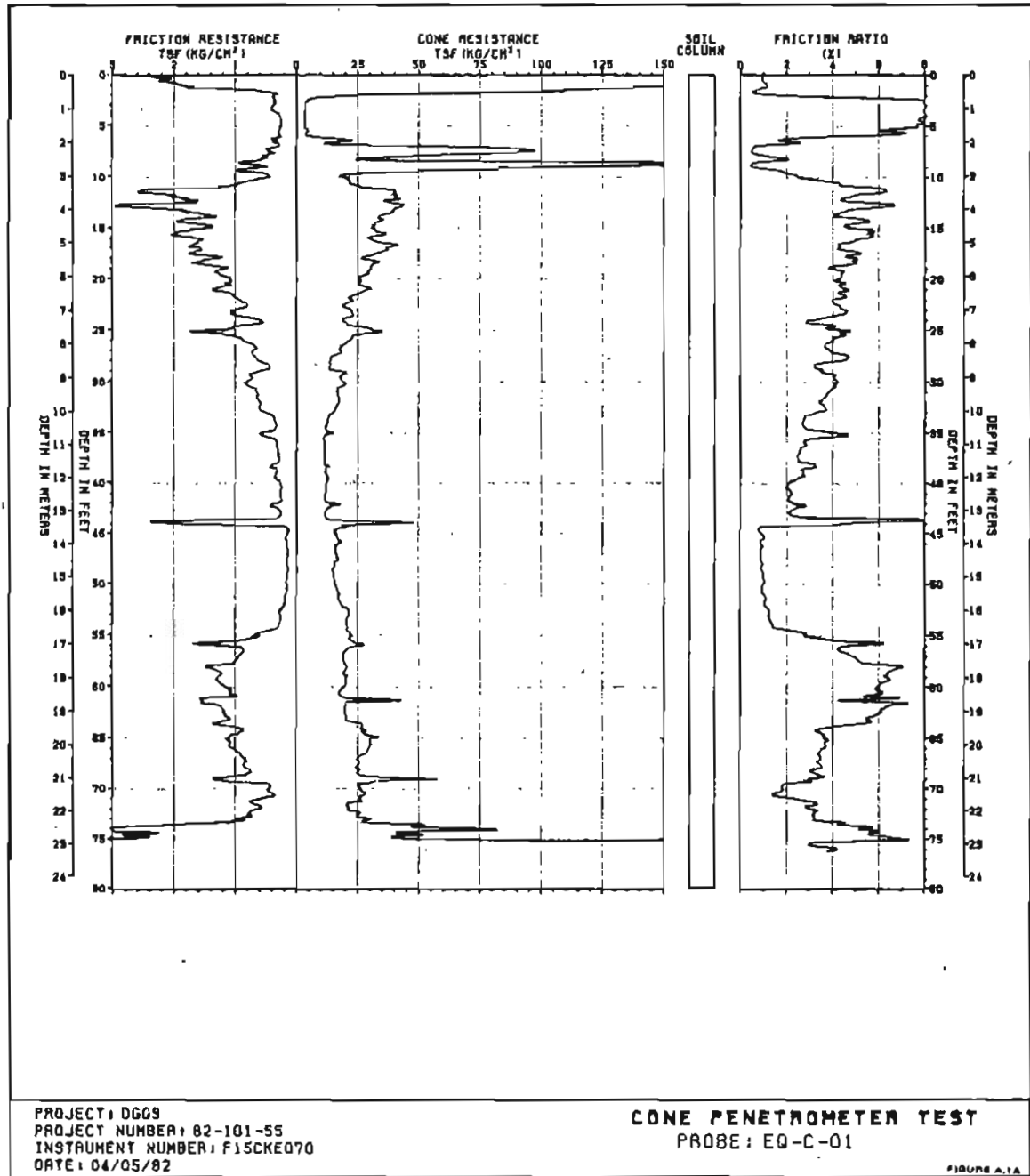


Figure 7. Computer-generated CPT strip charts obtained April 5, 1982, for site EQ-1 (fig. 1).

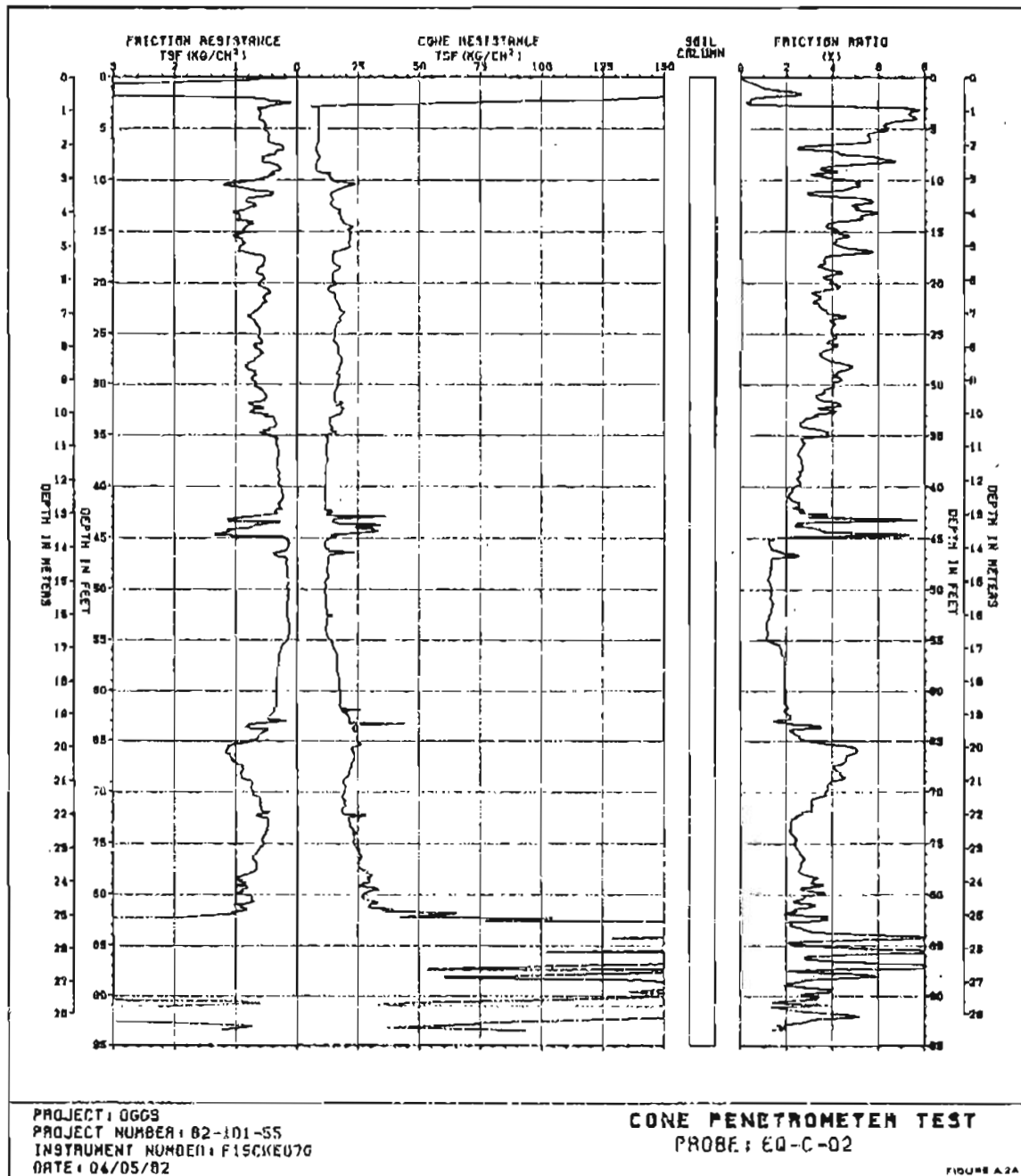


Figure 8. Computer-generated CPT strip charts obtained April 5, 1982, for site EQ-2 (fig. 1).

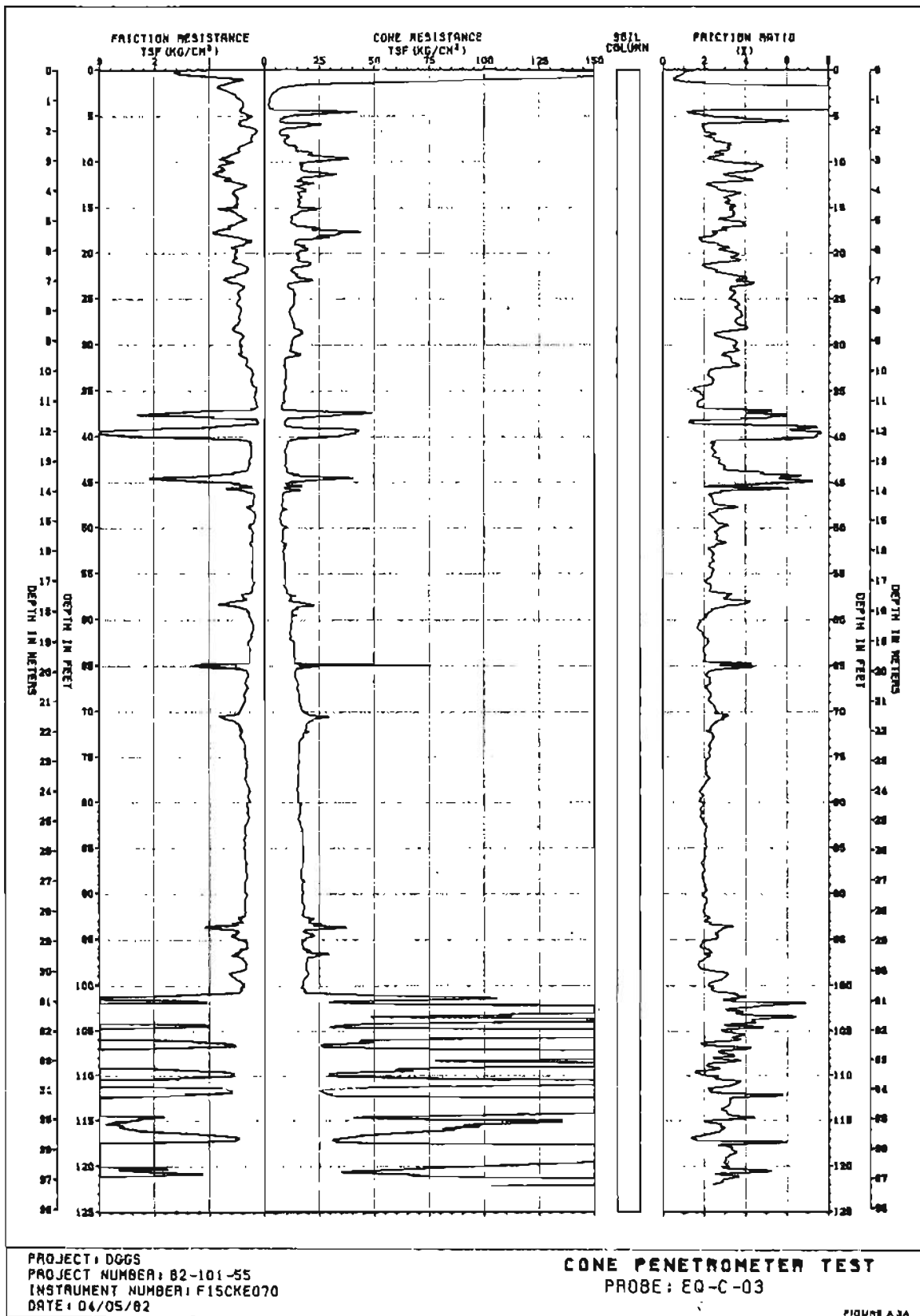


Figure 9. Computer-generated CPT strip charts obtained April 5, 1982, for site EQ-3 (fig. 1).

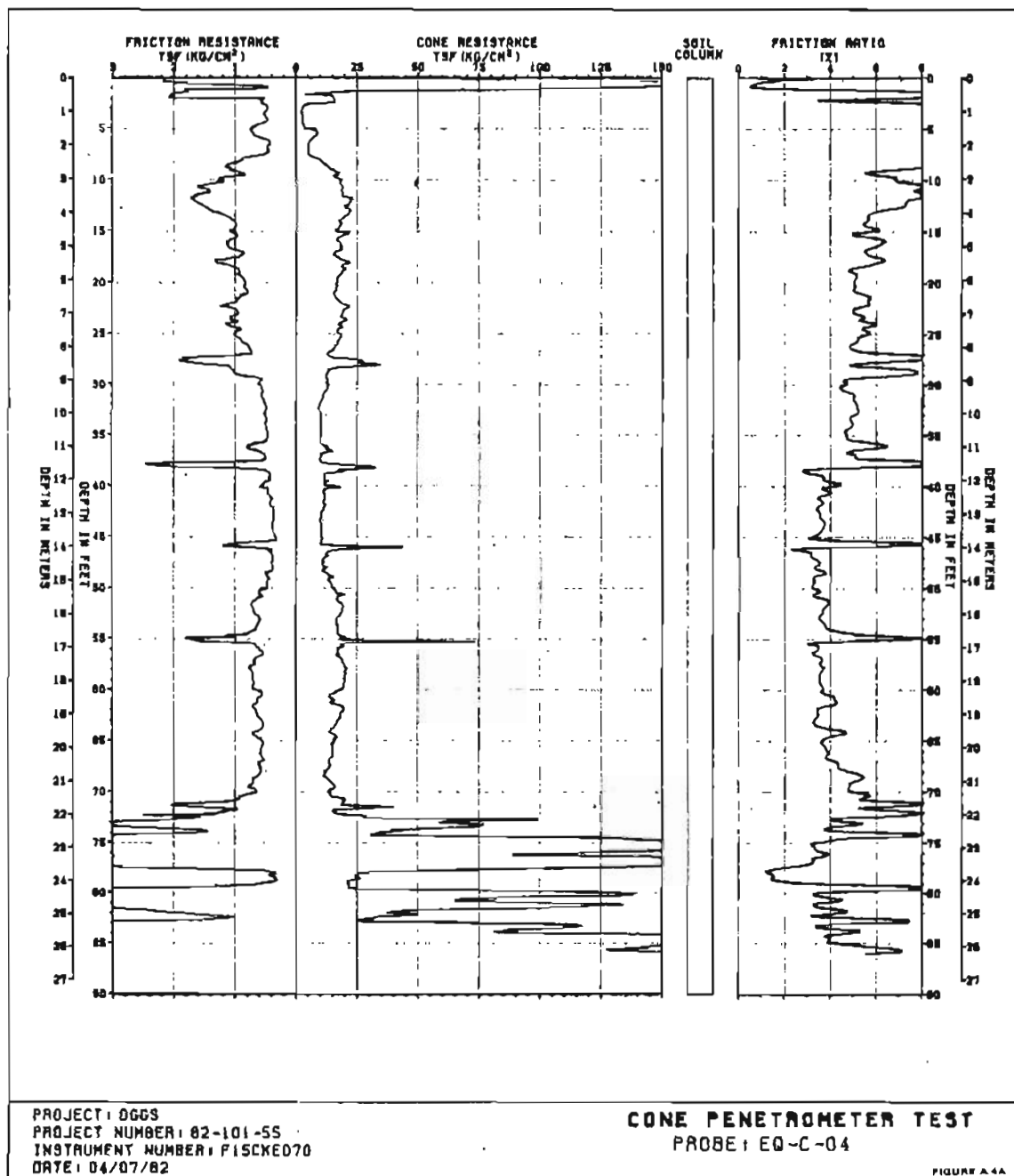


Figure 10. Computer-generated CPT strip charts obtained April 7, 1982, for site EQ-4 (fig. 1).

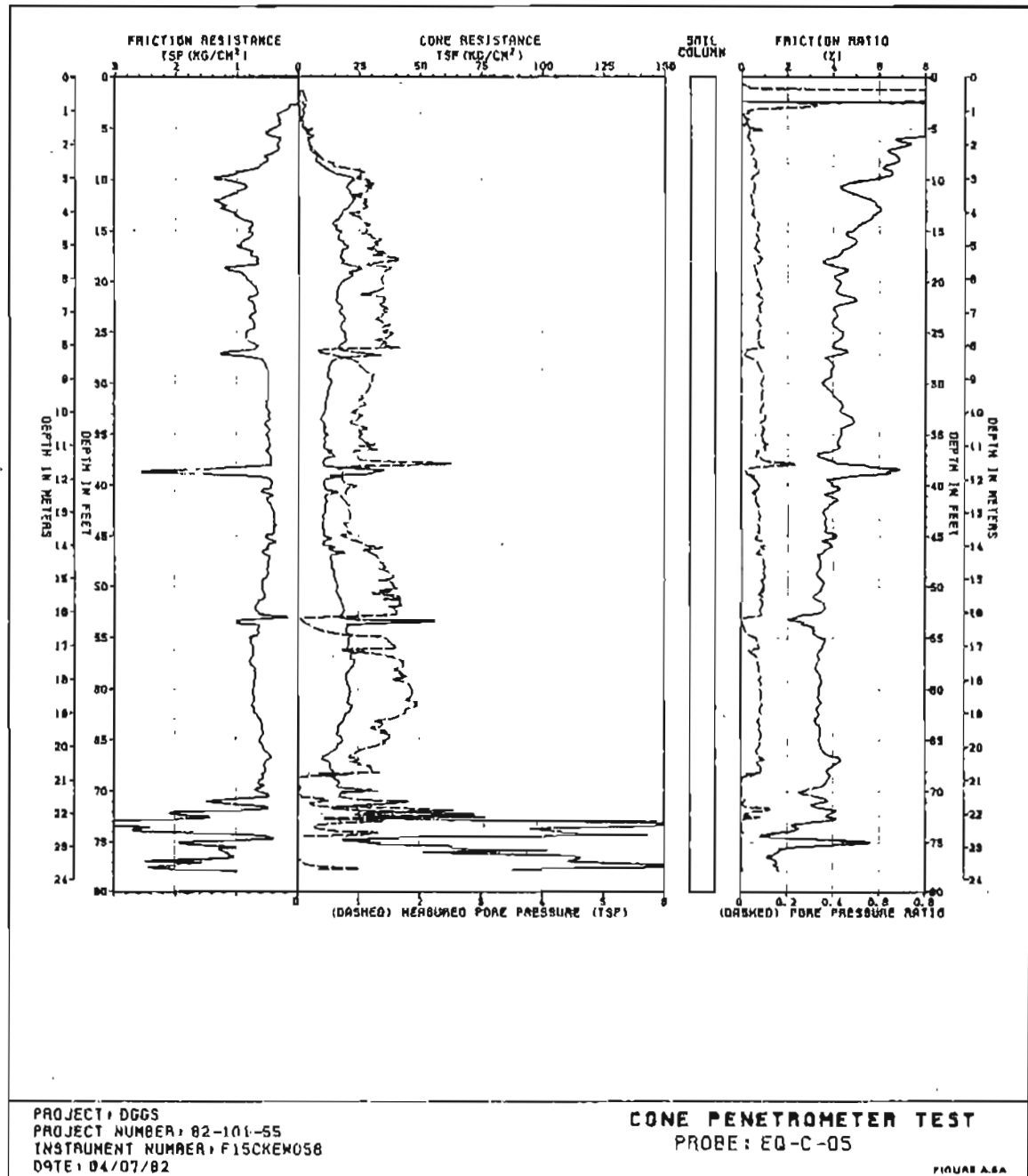


Figure 11. Computer-generated CPT strip charts obtained April 7, 1982, for site EQ-5 (fig. 1).

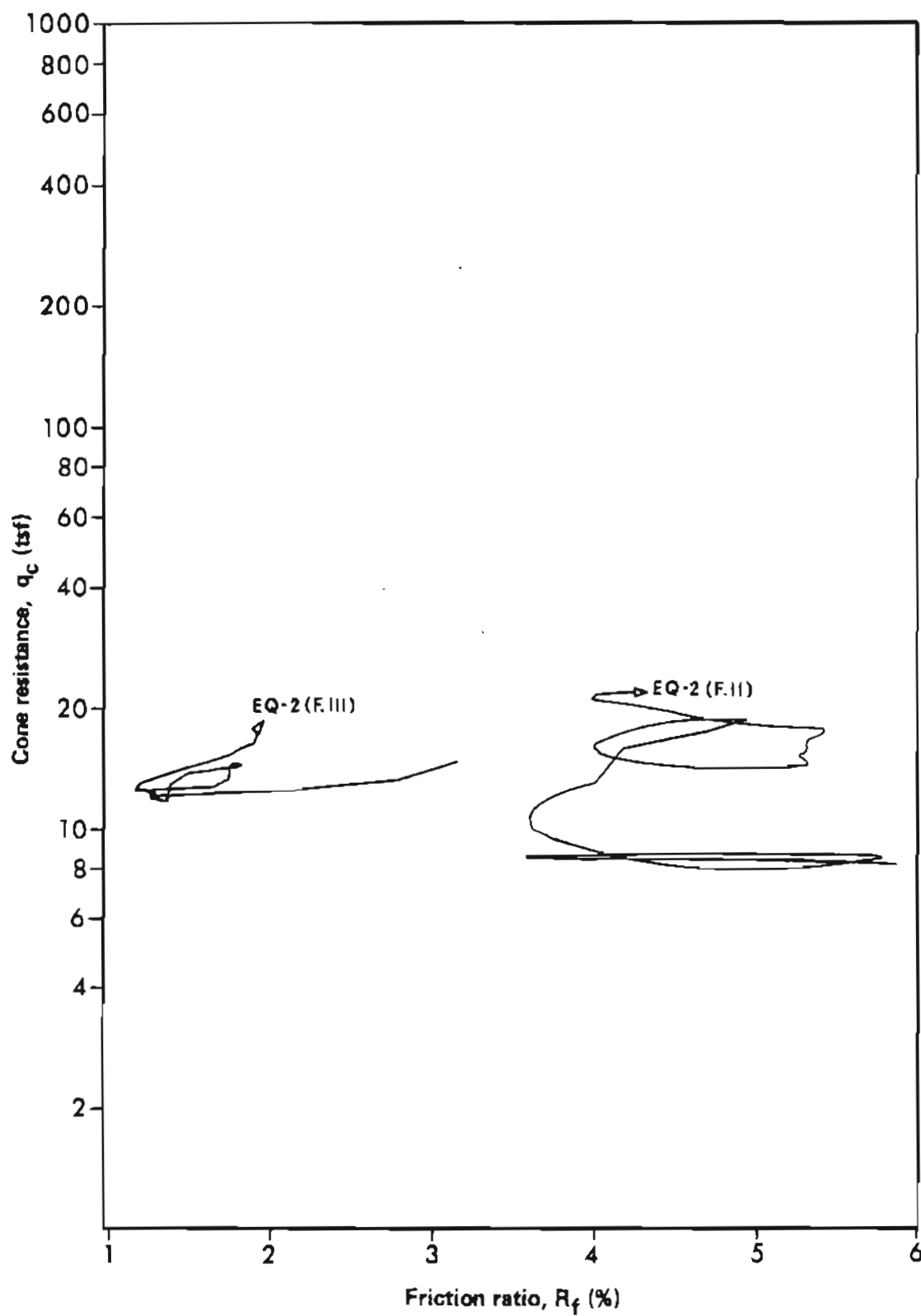


Figure 12. Graph of cone resistance (q_c) vs. friction ratio ($R_f = f_s/q_c$) for facies F.II and F.III. The computer-generated tracks are representative of those obtained for each facies from each site and were used to define the domains of figure 13.

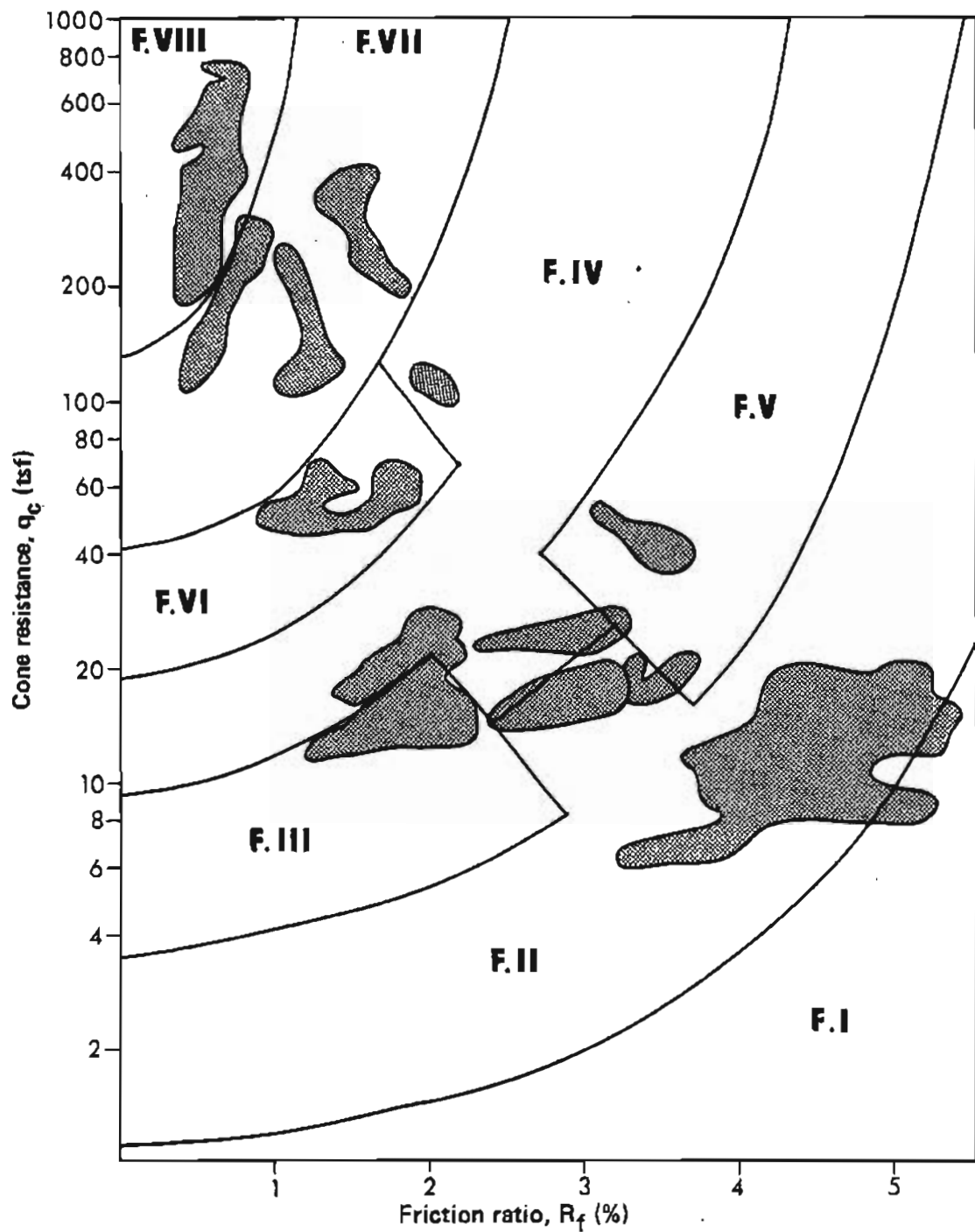


Figure 13. Graph of cone resistance (q_c) vs. friction ratio ($R_f = f_s/q_c$); derived from CPT data showing soil-behavior domains for facies of the Bootlegger Cove Formation.

Numerous efforts have been made to correlate CPT data to in-situ shear strength (Sanglerat, 1972; Lunne and others, 1976; Schmertmann, 1978). Because shear strength is of primary concern due to failure of cohesive facies in the Bootlegger Cove Formation, I attempted to approximate the undrained shear strength (S_u). Because penetration of the cone tip into undisturbed silts and clays is a bearing-capacity problem, most efforts employ a back-calculation technique that uses the classic bearing-capacity equation:

$$q_u = S_u N_c + \sigma_v$$

where q_u = ultimate bearing capacity
 S_u = undrained shear strength
 N_c = dimensionless bearing-capacity factor
 σ_v = total vertical stress

By setting q_u equal to q_c (from the CPT) a theoretical value of the shear strength can be determined:

$$S_u = (q_c - \sigma_v) / N_c$$

The primary difficulty is the selection of a proper value for N_c . Previous investigators used measured field and laboratory results for S_u and back-calculated N_c values that ranged from five (for high-sensitivity clays) to 25 (for over-consolidated dry clays). The possible error in arbitrarily selecting an N_c value and applying it to CPT data to determine shear strength is critical. For this project, an N_c value of 20 for high-friction-ratio silty clays was chosen based on field and laboratory test results of samples from borings near the CPT locations. The field tests included torvane and pocket-penetrometer tests. Torvane and unconfined compression tests were also performed on correlative samples in the laboratory. By comparing the results with the corresponding CPT-sounding log, the N_c factor was estimated based on both the above measurements and on previous measurements taken by Douglas (oral commun., 1983) on similar soils. After the estimated values of N_c were computed, the computer calculated the shear-strength values (S_u) shown in the appendix.

For comparative purposes, S_u was also calculated based on the hypothesis that the sleeve-friction value (f_s) represents a shear-strength value between the calculated undisturbed shear strength and the remolded shear strength (Schmertmann, 1971). A dimensionless constant of 1.10 was multiplied by the f_s values to derive the second set of S_u values tabulated in the appendix. Because of the present lack of theoretical understanding of the cone-sleeve-soil interaction and the remolding phenomena as the tip passes through a cohesive facies, the calculation of S_u based on CPT data should be regarded cautiously.

As previously mentioned, the standard-penetration test (SPT) is the more common method of assessing in-situ soil conditions. This method consists of driving a 50.8 mm-diam (2 in.) split-spoon sampler into the ground by dropping a 63-kg (140 lb) mass from a height of 760 mm (30 in.). The penetration resistance (N) is reported in number of blows to drive the sampler 305 mm (12 in.) into the soil. Because variation in N values can occur as a result of differences in equipment and technique of operators, methodology should be

specified. Nevertheless, N values are currently used as a basis for liquefaction-potential analyses throughout the United States. Bennett and others (1981) and Douglas and others (1981) have been successful in their attempts to correlate the penetration data derived from CPT and SPT techniques at a given site. On the basis of the relationships derived by Douglas and others (1981), we used a computer routine that generated a predicted equivalent SPT profile for each of the five sites using the CPT logs (figs. 14 through 18). Whereas actual SPT values are obtained with a sampler and therefore can only record a series of vertical data points with intervening data gaps, the CPT-equivalent technique provides a continuous, predicted SPT profile with respect to depth. All predictions were made using the following equation:

$$N = 12.5 E_D^{1.3}$$

where N is the predicted blow count and E_D is the energy expended during soil penetration of the SPT sampler. Constants relating the energy-dissipation function, E_D , to the SPT values obtained in carefully monitored borings in the Bootlegger Cove Formation elsewhere in Anchorage were evaluated. The results show a good correlation between predicted and real SPT values when a low-energy, trip-hammer technique is used. Correlation of the profiles in figures 14 to 18 is most applicable to liquefaction-potential analyses of the noncohesive facies F.VI and F.VII based on the trip-hammer penetration test. Constants relating N and E_D are dependent on the energy-transfer efficiency of the specific SPT hammer-anvil-rod-sampler system used. If another sampler system is used in gathering SPT data, a conversion factor may be required to correlate the data with the profiles in figures 14 to 18. This calibration of measured and predicted SPT values specific to equipment has been successfully used by Douglas and others (1981).

The piezo-cone-profile results (fig. 11) should be viewed conservatively, but analogies can be drawn from the limited experimental and field data (Douglas, oral commun., 1982) that have been published. The dramatic rise in pore pressure at a depth of about 2.6 m (8 ft) marks the phreatic surface at this station (site EQ-5, fig. 1). The correlation of a pore-pressure spike with a facies F.VI bed at 12.4 m (38 ft) reflects the characteristic pore-pressure buildup in a sandy silt as cone stress is applied. In contrast, the well-sorted sands (F.VII) at 8.8 m and 17.5 m (27 and 53 ft) are thin but can more efficiently dissipate pore pressures due to high permeability and lateral continuity.

CALIBRATION AND CORRELATION

The character of each engineering-geology facies of the Bootlegger Cove Formation has been carefully documented in several areas in Anchorage (Updike and Carpenter, 1985; Updike, 1982, 1985; Updike and others, 1982; Updike and Ulery, 1985). On the basis of field and laboratory inspection of numerous samples of each facies, the CPT profiles can be calibrated to distinguish these facies, and the following characteristics can be applied to other CPT profiles of the formation. Facies F.I is not listed because true clay layers are generally too thin to be distinguished on a CPT profile.

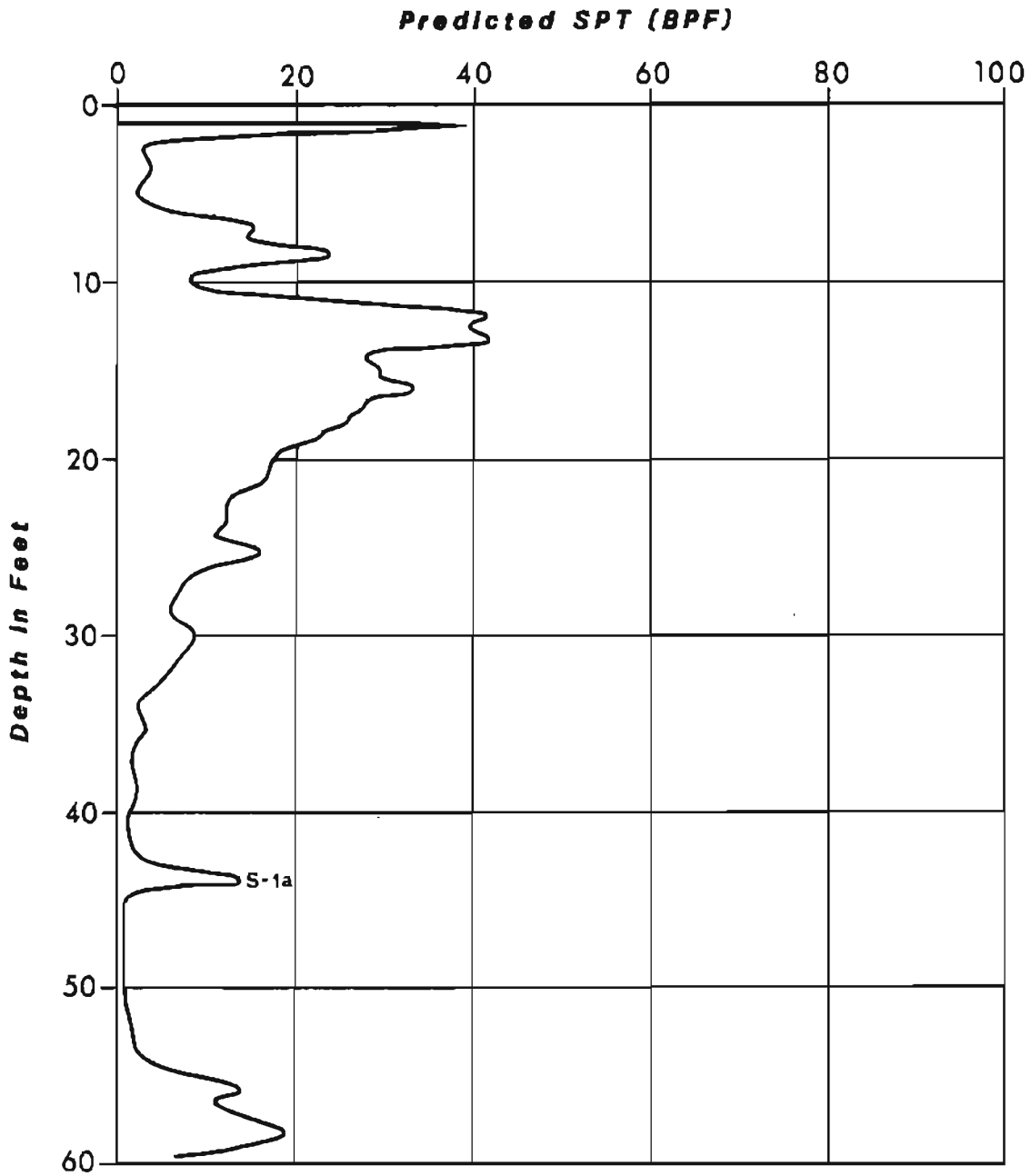


Figure 14. Graph showing SPT profile for site EQ-1 as predicted from CPT data. Sand at S-1a is plotted on figure 24.

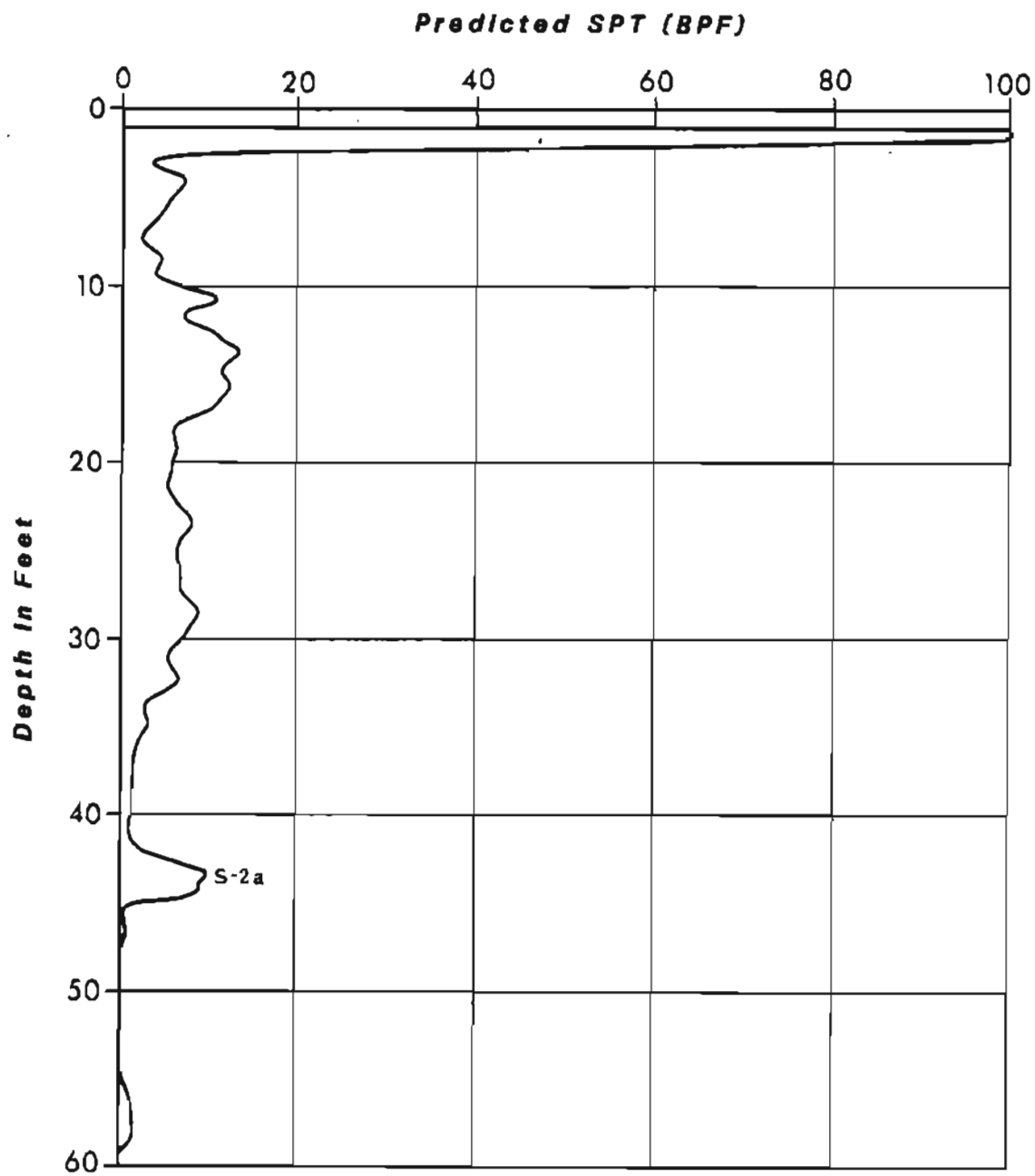


Figure 15. Graph showing SPT profile for site EQ-2 as predicted from CPT data. Sand at S-2a is plotted on figure 24.

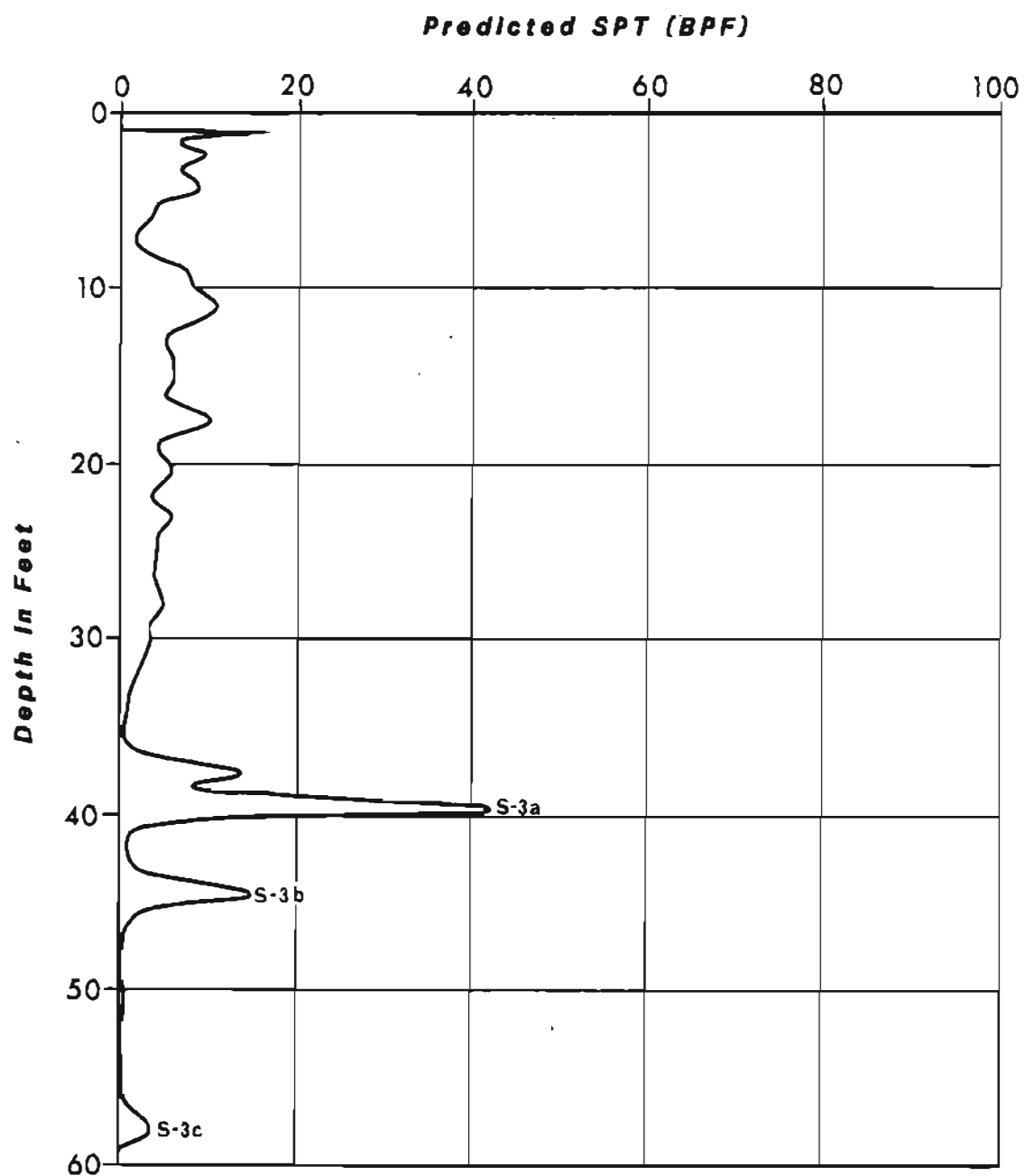


Figure 16. Graph showing SPT profile for site EQ-3 as predicted from CPT data. Sands at S-3a, S-3b, and S-3c are plotted on figure 24.

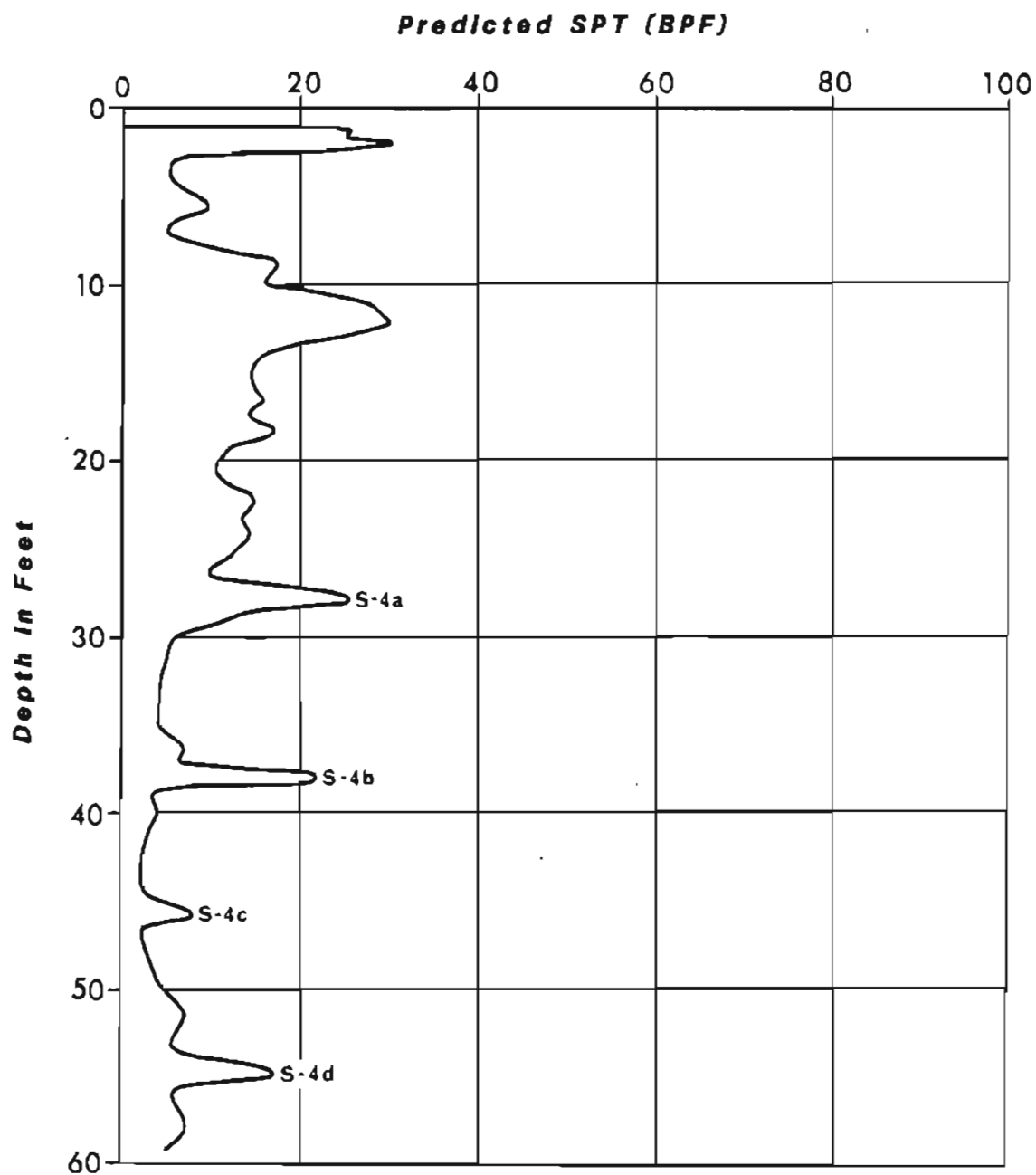


Figure 17. Graph showing SPT profile for site EQ-4 as predicted from CPT data. Sands at S-4a, S-4b, S-4c, and S-4d are plotted on figure 24.

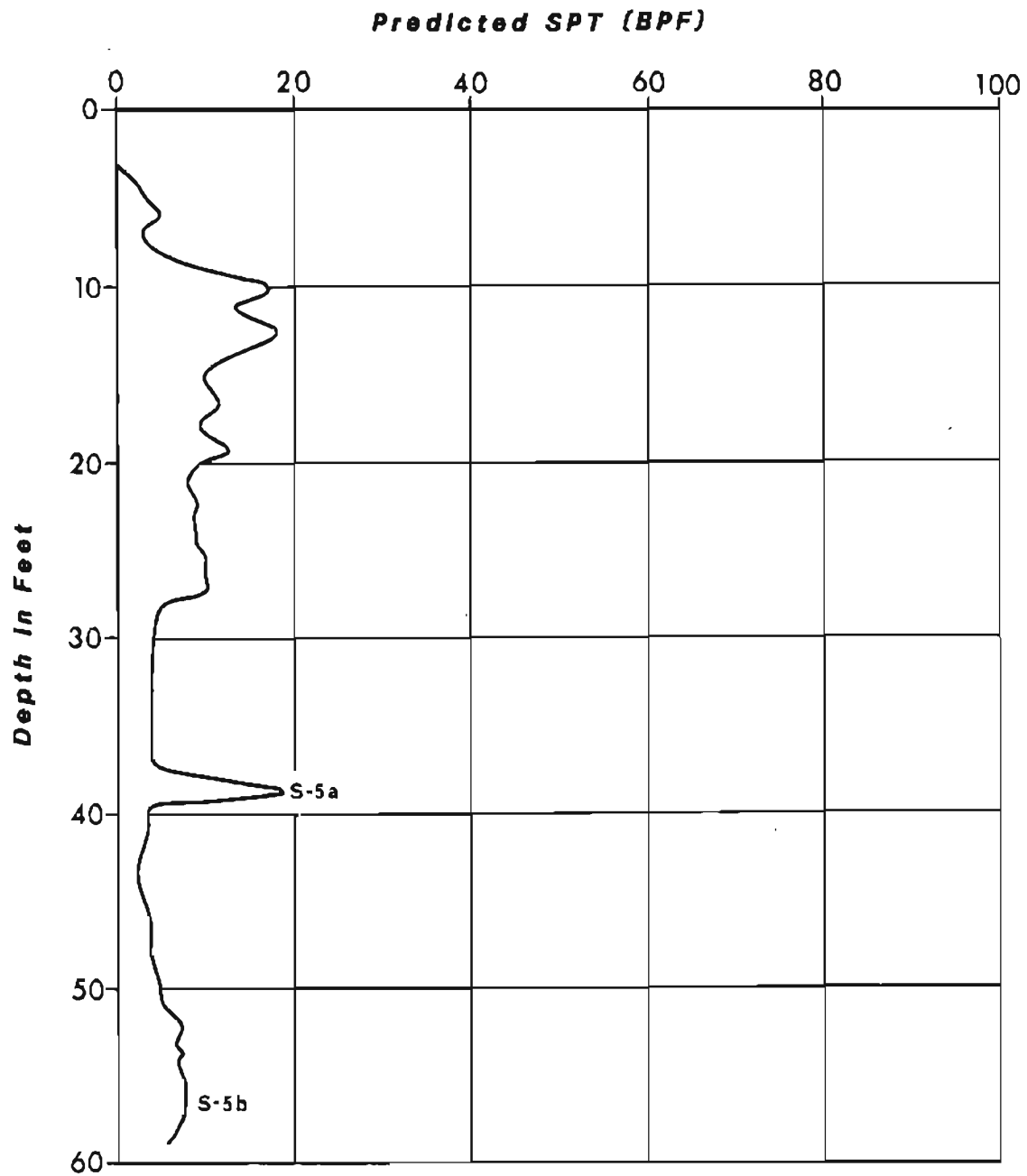


Figure 18. Graph showing SPT profile for site EQ-5 as predicted from CPT data. Sands at S-5a and S-5b are plotted on figure 24.

- F.II Profile relatively smooth with minor spikes due to sandy-silt layers.
- q_c = less than 25 ton/ft²
 f_s = less than 1 ton/ft²
 R_f = 2 to 4 percent
- F.III Profile very smooth with vertical slope.
- q_c = less than 15 ton/ft²
 f_s = less than 0.4 ton/ft²
 R_f = less than 2 percent
- F.IV Profile very erratic with numerous spikes; often slopes toward the 'O' line with increasing depth.
- q_c = 15 to 35 ton/ft²
 f_s = 1 to 2 ton/ft²
 R_f = 3 to 7 percent
- F.V Profile erratic but often bell-shaped; spikes due to sand and stones.
- q_c = 25 to 30 ton/ft²
 f_s = 0.5 to 2.0 ton/ft²
 R_f = 3 to 7 percent
- F.VI Profile shows abrupt spikes on three curves.
- q_c = 25 to 50 ton/ft²
 f_s = greater than 1 ton/ft²
 R_f = greater than 4 percent
- F.VII Profile shows abrupt spike on q_c , minor spike on f_s , trough on R_f .
- q_c = greater than 100 ton/ft²
 f_s = less than 2 ton/ft²
 R_f = less than 1 percent

Other geologic units found by the CPT sounding also produce distinctive profiles. The peat and loose silt that overlie the Bootlegger Cove Formation yield very low q_c and f_s curves, and the resultant R_f is very high. The upper meter of soil was frozen during the soundings and produced spikes that were off the scale for q_c and f_s with a resultant R_f near zero. Sediments below the Bootlegger Cove Formation were also generally off the scale for q_c and f_s ; numerous troughs indicate silt interbeds. Friction ratios for these deep soils are usually greater than 2 percent.

Seven geotechnical boreholes previously drilled (Shannon and Wilson, 1964) near the CPT sites were selected for stratigraphic correlation. The CPT soundings were calibrated according to the facies criteria discussed above. A cross section (fig. 1) that passes through CPT sites EQ-1, EQ-2, and EQ-3 and is near the chosen boreholes was selected. The borehole logs were calibrated using the previously established engineering-geology-facies criteria of Updike and Carpenter (1985). The resultant stratigraphic-correlation chart (fig. 19) shows an excellent match between major units.

Three main stratigraphic units are recorded on the profiles: a) very late Pleistocene to Holocene peat, silt, and loose sand, b) Bootlegger Cove Formation, and c) Pleistocene (Knik Glaciation?) diamicton. The uppermost unit varies from 0.6 m (2 ft) to 3.3 m (10 ft) in thickness; the top 2 to 2.5 ft is seasonally frozen. The Bootlegger Cove Formation consistently increases in thickness from 21 m (68 ft) in the west to 34 m (104 ft) to the southeast over a horizontal distance of approximately 500 m (1,525 ft). The unit below the Bootlegger Cove Formation is far more consolidated than the formation directly above so that penetration was very difficult and resistance quickly exceeded the equipment's 20-ton capacity. Borehole logs indicate that this unit is several tens of feet thick and varies from overconsolidated clayey silt to sandy gravel. The abrupt transition in q_c and f_s values at the contact between the Bootlegger Cove Formation and these older sediments supports the interpretation that the contact marks a substantial time hiatus. The high end-bearing values below the contact also indicate either substantially higher lithostatic loads in pre-Bootlegger time or a long time interval in which these older sediments were exposed to dessication and weathering. This would most adequately be explained by a pre-Naptowne Glaciation age for the deposits.

Within the Bootlegger Cove Formation, all facies are distinguishable with the exception of F.I, which is generally only identifiable in laboratory samples. The typical sequence throughout the series of holes and CPT soundings is: a) sands of F.VI and F.VII at the top of the formation; b) a thick sequence of F.IV, which decreases in strength with increasing depth; c) a uniform sequence of F.II that becomes progressively thicker to the southeast and within which both F.III beds and thin intercalated layers of F.VI occur; d) a consolidated F.V layer that marks the base of the formation in the west, but grades into F.II and F.IV to the southeast (fig. 19).

The in-situ undrained shear strengths derived from the CPT data are correlated with S_u values obtained in the laboratory on core samples in figures 20 through 23. The cores were obtained from boreholes drilled and tested in 1964 (Shannon and Wilson, 1964). Thus, the quality of the cores and

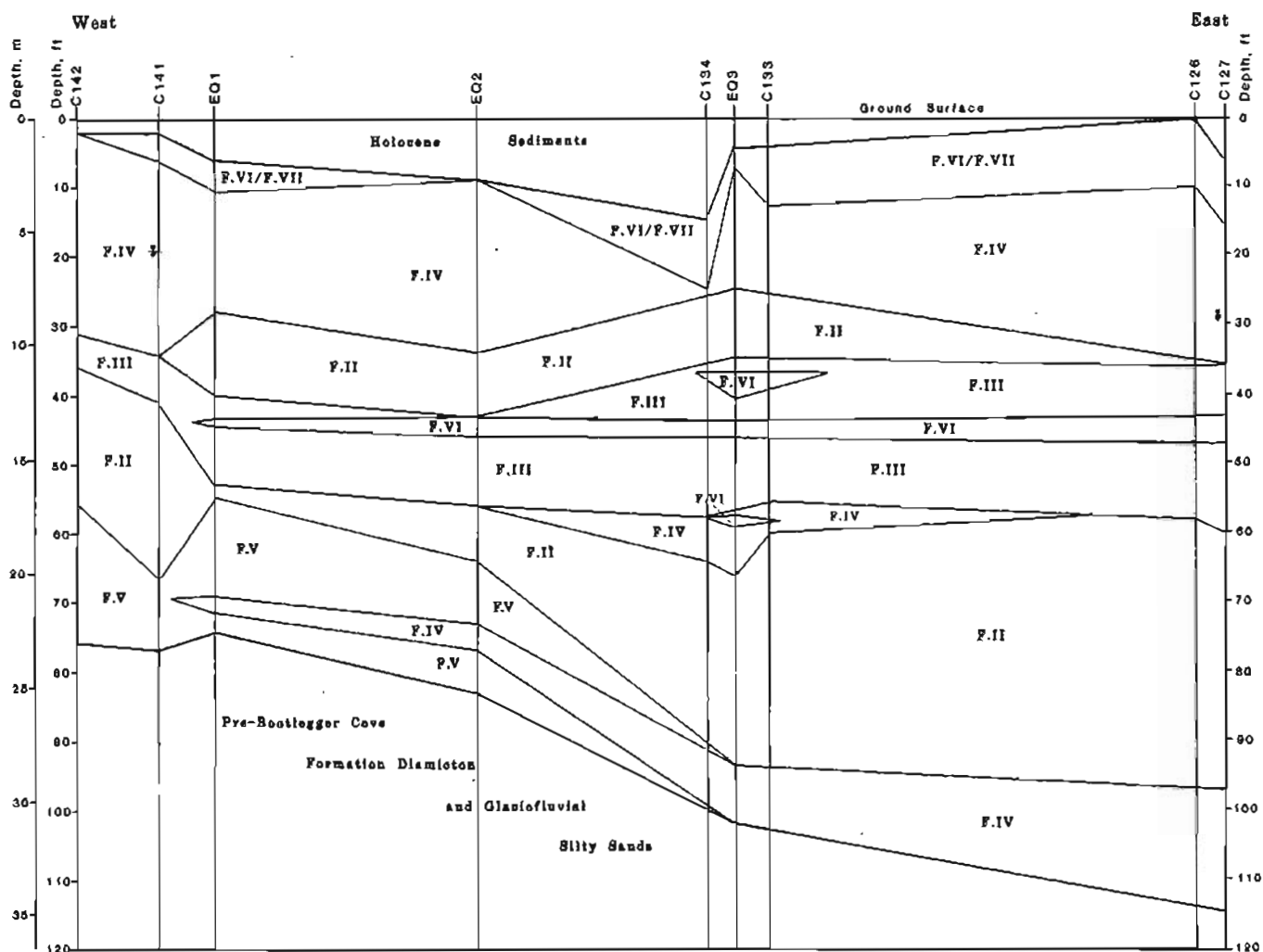


Figure 19. East-west cross section based on geotechnical boreholes and cone-penetration soundings in the vicinity of Earthquake Park, Anchorage (see fig. 1).

the technique of laboratory testing are not verifiable. Each figure shows selected CPT data points vs. depth and all laboratory data points. General variation trends in shear strength can be equated between the three series of points (lab S_u , S_u based on f_s , and S_u based on q_u and σ_v). However, there is a significant disparity between values at several depths, particularly where estimated S_u is greater than 0.5 ton/ft². Also, there is generally a closer agreement between lab values and f_s values than with q_u -derived values. The sleeve-friction measurement appears to consistently provide a more conservative S_u . The tendency for the f_s -derived values to be lower than laboratory-derived S_u 's may reflect the unknown effect of soil remolding as the soil is penetrated. Because the accuracy of the laboratory techniques cannot be documented, the laboratory-derived S_u values must be regarded conservatively. Further, the CPT-derived values are essentially continuous throughout the

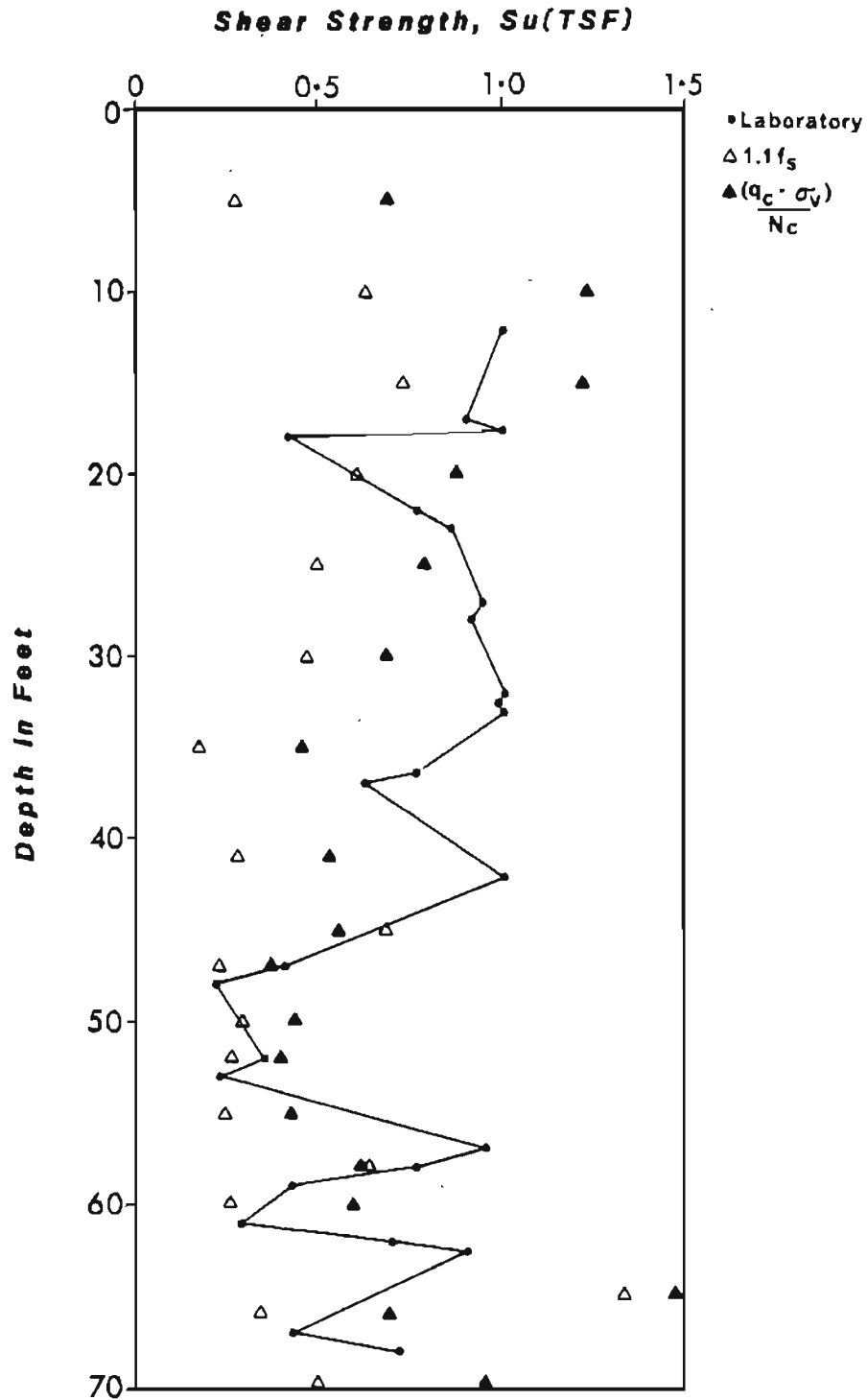


Figure 20. Graph of undrained shear strength vs. depth. Empirical values derived from the CPT for site EQ-3 are compared with laboratory values from boreholes C-133 and C-134 (fig. 1).

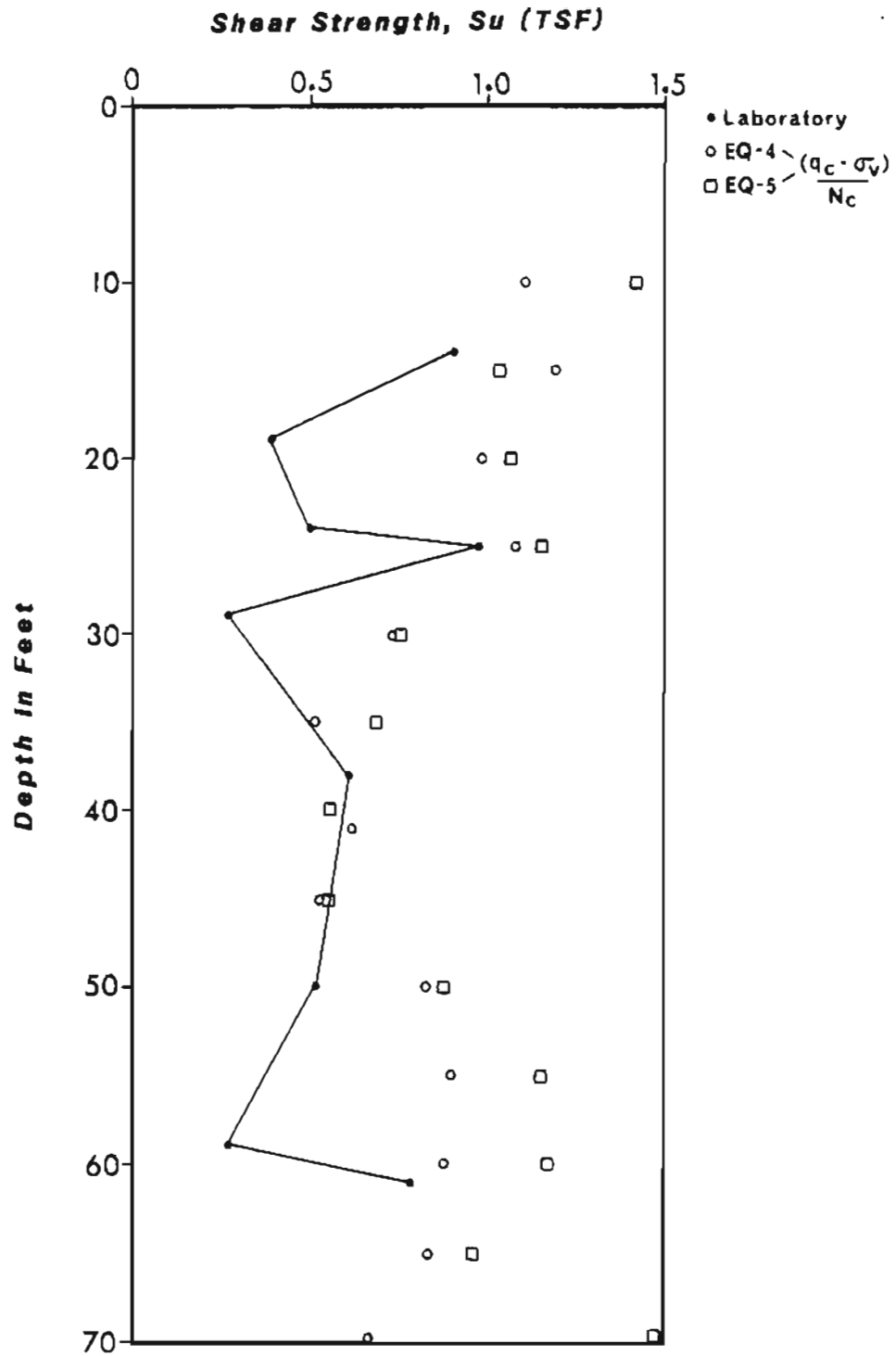


Figure 21. Graph of undrained shear strength vs. depth. Empirical values derived from the CPT for sites EQ-4 and EQ-5 (using the equation $S_u = f_u \times 1.10$) are compared with laboratory values from borehole C-140 (fig. 1).

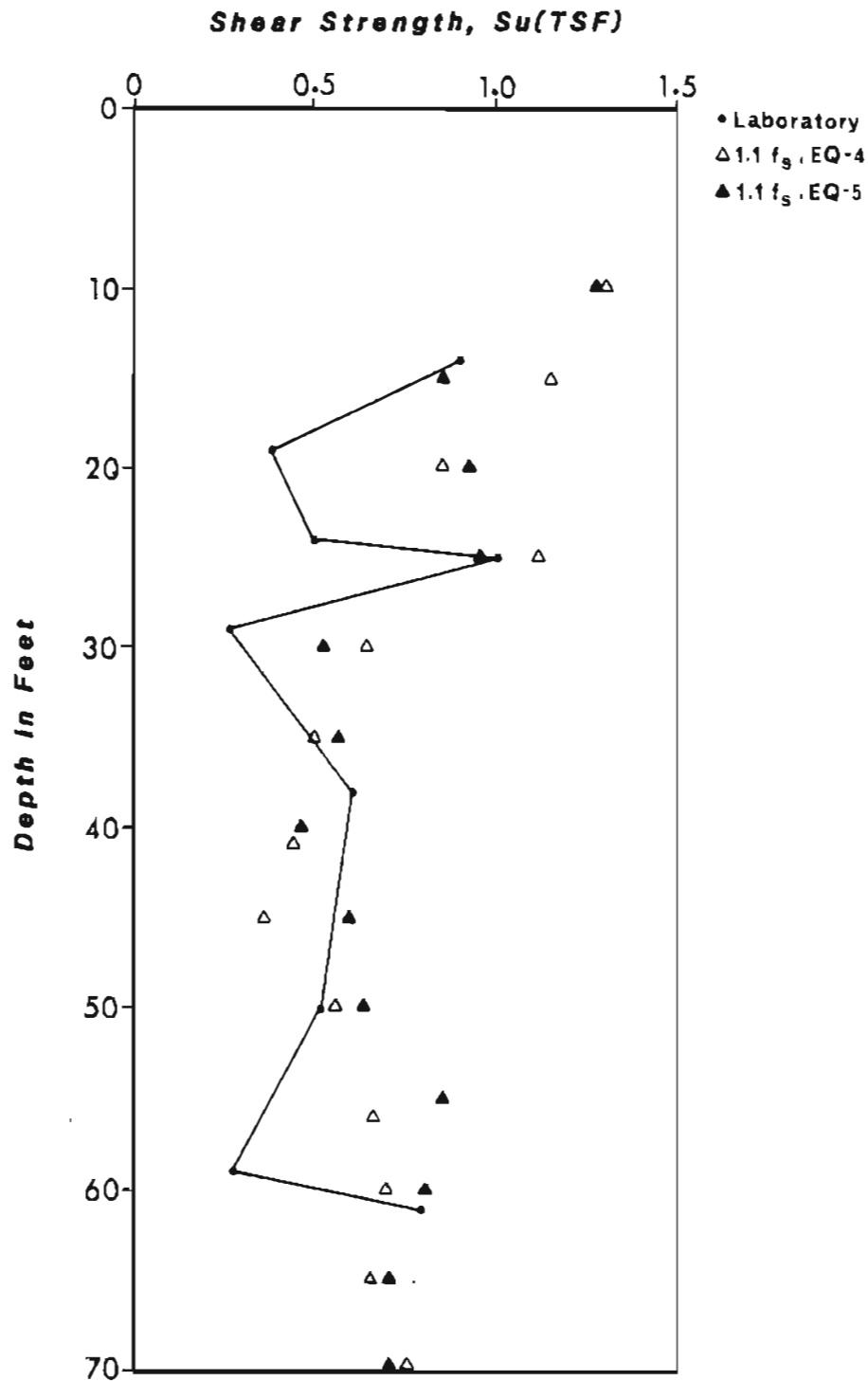


Figure 22. Graph of undrained shear strength vs. depth. Empirical values derived from the CPT for sites EQ-4 and EQ-5 [using the equations $S_u = (q - \sigma_v' / N_c)$] are compared with laboratory values from borehole C-40 (fig. 1).

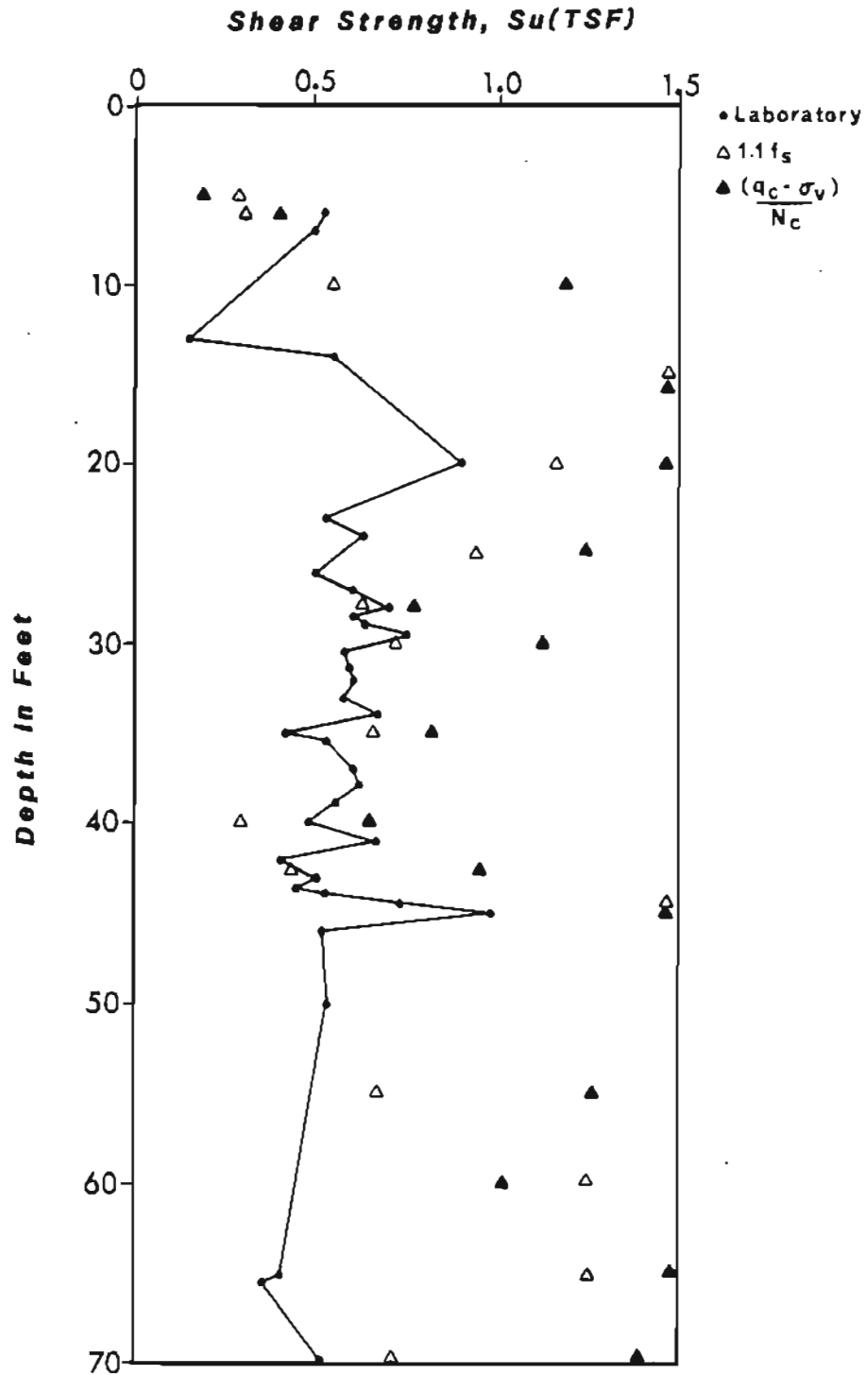


Figure 23. Graph of undrained shear strength vs. depth. Empirical values derived from the CPT for site EQ-1 are compared with laboratory values from boreholes C-141 and C-142 (fig. 1).

length of the sounding under constant testing conditions, whereas the laboratory tests are only provided for specific test points within a core. Therefore, there is more chance for atypical test results on laboratory cores that have unknown variables, such as original sample disturbance, faulty stratigraphic control, loss of sample moisture, or disturbance in the lab. One must conclude that although the CPT method cannot replace the laboratory tests, it can complement the limited laboratory values with a more comprehensive profile of empirical shear strengths. The closest correlation of S_u values between the three techniques is provided by those soils that have very low shear strengths, and whose soil stability is of most concern. Thus, where the strength values are most needed from the CPT, they seem to be most reliable. The greater disparity at higher S_u values may reflect the introduction of increasing amounts of granular particles that would enhance the cone-bearing values (for the q_u -based calculations) and reduce the sleeve-friction values in the soil. In facies F.IV and F.V, the laboratory value is more accurate.

CONCLUSIONS

Although the logs recorded by the CPT system correlate very well with the geotechnical-borehole logs, they result from continuous soundings and yield a more detailed characterization of the soil than can be attained from a sampling technique. The CPT approach is most effective in a testing program complemented by conservative drilling, sampling, and laboratory testing. The CPT system provides a comprehensive and detailed picture of the subsurface geology; aids in determining what soil units should be sampled during a subsequent drilling program; acquires data on soil units that would be very difficult to sample; decreases the time required to investigate a site by limiting the amount of drilling needed; and substantially reduces the cost of geotechnical-site evaluation without sacrificing quality.

Correlation of borehole logs and CPT profiles in the Earthquake Park area provides a three-dimensional stratigraphic picture consistent with the previously proposed model of an ice-marginal deltaic regime that extends into a quiet-water depositional basin to the east. The early phase of this system included the accumulation of facies F.V ice-rafted debris that grades eastward into more uniformly fine-textured clayey silts with interbedded silty fine sands (F.IV). This time interval, represented by facies F.II and F.III, was probably a period of marine deposition and should be confirmed by the presence of marine fossils. The climax of basin deposition consisted of more varied textures of clays, silts, and sands interbedded in a restricted basin where the fresh-water influence from adjacent glaciers affected sedimentation rates and energy. The sequence F.IV should yield fresh-water microfauna. The top of the formation is marked by a discontinuous bed of silty fine sand (F.VI) to medium sand (F.VII) that represents basin-water drainage to expose fan-delta sediments.

The Turnagain Heights landslide was a result of failure within the facies F.III zone (fig. 19), probably due to fabric collapse of the sensitive, silty clays. Facies F.III is present throughout the study area, but significantly increases in thickness from 3.3 m (10 ft) (northwest) to 9 m (28 ft) (southeast). This zone of potential failure will vary in elevation from less than

+2 m (5 ft) to about +12 m (35 ft), and therefore geotechnical testing for design work should evaluate soils to a depth of about 22 m (65 ft). The silty fine sand beds (F.VI) within facies F.III were poorly recorded in the boreholes, but are obvious in the CPT soundings. These sands may be responsible for the sensitivity of the adjacent silts and clays by functioning as confined aquifers whose waters leach salts from the surrounding finer sediments.

For moderate to high shear-strength soils, the CPT empirical derivations of S_u are less than adequate. However, at low S_u values, the correlation between laboratory and CPT values is quite close, which strongly supports my hypothesis that the sensitive facies have strength properties identical to those that existed in 1964. A preliminary evaluation of liquefaction susceptibility for the facies F.VI silty sands, using the SPT-equivalent profiles (figs. 14 through 18) to give N values, was applied using the technique of Nishiyama and others (1977). The N values used in the plot of SPT vs. depth (fig. 24) were modified by the addition of 7.5 to the raw

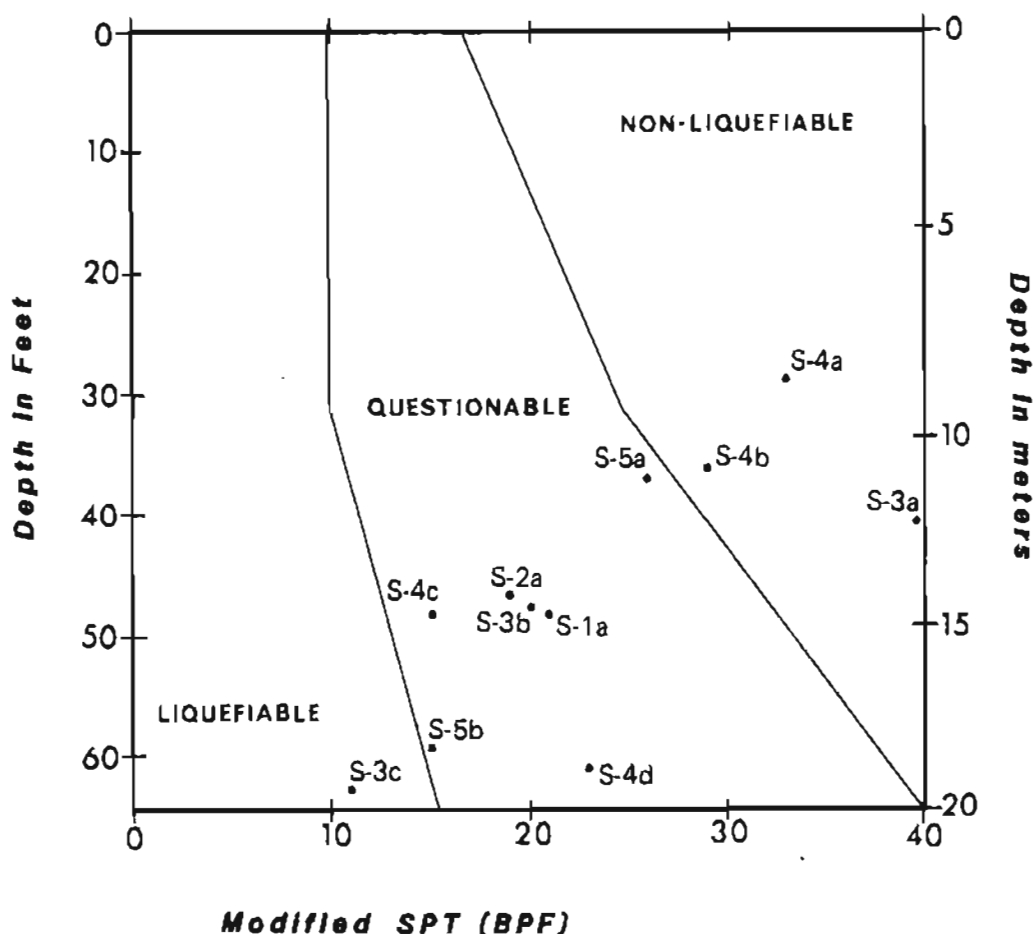


Figure 24. Graph of SPT (blows per ft) vs. depth, with field of liquefaction susceptibility (from Nishiyama and others, 1977). Data points are from predicted SPT profiles in figures 14 to 18 for sands and silty sands. SPT values have been modified for silty sands as recommended by Seed and Idriss (1981).

numbers taken in figures 14 through 18. This follows the suggestion of Seed and Idriss (1981) that the 7.5 factor is required for silty sands in order to enter the SPT plot. The resultant plot indicates that facies F.VI zones are either questionable or nonliquefiable. More advanced techniques of liquefaction-potential analyses were not used because I do not feel that a reliable CPT-SPT analog has been derived for Anchorage area soils. However, the plot gives some support to my hypothesis that the Turnagain Heights landslide was a result of sensitive, clayey silt collapse rather than sand liquefaction (Updike, 1983). The abrupt termination (to the west) of the 1964 slide can be attributed to the rapid thinning of facies F.III in that direction. This thinning may be a result of the subtle change in depositional regime near the western source area (that is, a change in soil fabric even though grain-size distribution is similar), or to the pinching out of the facies F.VI sands that may have enhanced sensitivity of F.II silty clays due to leaching in Holocene time and resulted in the F.III facies.

ACKNOWLEDGMENTS

This project was supported by funds provided by a cooperative agreement between DGGs and the U.S. Geological Survey under the U.S. Geological Earthquake Hazards Reduction Program. Personnel of Earth Technology Corporation were essential to the success of this investigation and include Bruce Douglas, Brenda Meyer, George Edmonds, and Richard Renaud. T.L. Youd (U.S. Geological Survey) helped define the scope of the project. R.A. Combellick (DGGs) provided a technical review of the manuscript, and C.A. Ulery (DGGs) assisted in the field and with the cartography.

REFERENCES CITED

- Barnwell, W.W., George, R.S., Dearborn, L.L., Weeks, J.B., and Zenone, Chester, 1972, Water for Anchorage, an atlas of the water resources of the Anchorage area, Alaska: City of Anchorage and the Greater Anchorage Area Borough, 77 p.
- Begeman, H.K., 1965, The friction jacket cone as an aid in determining the soil profile: International Conference on Soil Mechanics and Foundation Engineering, Proceedings, 6th, v. 1, p. 17-20.
- Bennett, J.J., Youd, T.L., Harp, E.L., and Wieczorek, G.F., 1981, Subsurface investigation of liquefaction, Imperial Valley Earthquake, California, October 15, 1979: U.S. Geological Survey Open-file Report 81-502, 83 p.
- Brown, L.D., Reilinger, R.E., Holdahl, S.R., and Balzaks, E.I., 1977, Post-seismic crustal uplift near Anchorage, Alaska: Journal of Geophysical Research, v. 82, p. 3369-3378.
- Cederstrom, D.J., Trainer, F.W., and Waller, R.M., 1964, Geology and ground-water resources of the Anchorage area, Alaska: U.S. Geological Survey Water Supply Paper 1773, 108 p.
- Douglas, B.J., and Olsen, R.S., 1981, Soil classification using electric cone penetrometer: St. Louis, Missouri, American Society of Civil Engineers Special Technical Publication, 1981, 19 p.
- Douglas, B.J., Olsen, R.S., and Martin, G.R., 1981, Evaluation of the cone penetrometer test for SPT-liquefaction assessment: American Society of Civil Engineers Preprint 81-544, 14 p.

- Hansen, W.R., 1965, Effects of the earthquake of March 27, 1964, at Anchorage, Alaska: U.S. Geological Survey Professional Paper 542-A, p. A1-A68.
- Karlstrom, T.N.V., 1964, Quaternary geology of the Kenai Lowland and glacial history of the Cook Inlet region, Alaska: U.S. Geological Survey Professional Paper 443, 69 p.
- Kerr, P.R., and Drew, I.M., 1965, Quick clay movements, Anchorage, Alaska: Springfield, Virginia, National Technical Information Service, Document AD630-111, 133 p.
- _____, 1968, Quick-clay slides in the U.S.A.: Engineering Geology International Journal, v. 2, p. 215-238.
- Long, Erwin, and George, Warren, 1966, Buttrass design earthquake-induced slides: Conference on Stability and Performance of Slopes and Embankments, Berkeley, California, Soil Mechanics and Foundations Division, American Society of Civil Engineers, p. 657-671.
- Lunne, T., Eide, O., and de Ruiter, J., 1976, Correlations between cone resistance and vane shear strength in some Scandanavian soft to medium stiff clays: Canadian Geotechnical Journal, no. 13, p. 430-441.
- Miller, R.D., and Dobrovolsky, Ernest, 1959, Surficial geology of Anchorage and vicinity, Alaska: U.S. Geological Survey Bulletin 1093, 128 p.
- Nishiyama, H., Yahagi, K., Nakagawa, S., and Wada, K., 1977, Practical method of predicting sand liquefaction: International Conference on Soil Mechanics and Foundation Engineering, 9th, Tokyo, Japan, Proceedings, v. 2, p. 305-308.
- Reger, R.D., and Updike, R.G., 1983, Upper Cook Inlet region and the Matanuska Valley, in Pêwé, T.L., and Reger, R.D., eds., Guidebook to permafrost and Quaternary geology along the Richardson and Glenn Highways between Fairbanks and Anchorage, Alaska: Alaska Division of Geological and Geophysical Surveys Guidebook 1, p. 185-263, scale 1:250,000, 1 sheet.
- Sanglerat, G., 1972, The penetrometer and soil exploration: New York, Elsevier, 488 p.
- Schmertmann, J.H., 1971, Discussion of the standard penetration test: Pan American Conference on Soil Mechanics and Foundation Engineering, 4th, San Juan, Puerto Rico, June 1971, Proceedings, v. 3, p. 90-98.
- _____, 1978, Guidelines for Cone Penetration Test, performance and design: U.S. Department of Transportation, Federal Highway Administration Report FHWA-TS-78-209, 145 p.
- Schmoll, H.R., and Dobrovolsky, Ernest, 1972, Generalized geologic map of Anchorage and vicinity, Alaska: U.S. Geological Survey Map I-787-A, scale 1:24,000.
- Searle, I.W., 1979, The interpretation of Begemann friction jacket cone results to give soil types and design parameters: European Conference on Soil Mechanics and Foundation Engineering, 7th, Brighton, England, Proceedings, v. 2, p. 265-270.
- Seed, R.B., 1968, Landslides during earthquakes due to soil liquefaction: Journal of Soil Mechanics and Foundations Division, American Society of Civil Engineers, v. 94, p. 1053-1122.
- _____, 1976, Evaluation of soil liquefaction effects on level ground during earthquakes: American Society of Civil Engineers Special Session on Liquefaction Problems in Geotechnical Engineering, Philadelphia, p. 1-104.

- Seed, H.B., and Idriss, I.M., 1981, Evaluation of liquefaction potential of sand deposits based on observations of performance in previous earthquakes: American Society of Civil Engineers Preprint 81-544, 21 p.
- Seed, H.B., and Wilson, S.D., 1967, The Turnagain Heights landslide, Anchorage, Alaska: Journal of the Soil Mechanics and Foundations Division, American Society of Civil Engineers, v. 93, p. 325-353.
- Shannon and Wilson, Inc., 1964, Report on Anchorage area soil studies, Alaska, to the U.S. Army Engineer District, Anchorage, Alaska: Seattle, Shannon and Wilson, Inc., 109 p.
- Trainer, F.W., and Waller, R.M., 1965, Subsurface stratigraphy of glacial drift at Anchorage, Alaska, in Geological Survey Research 1965: U.S. Geological Survey Professional Paper 525-D, p. D167-D174.
- Ulery, C.A., and Updike, R.G., 1983, Subsurface structure of the cohesive facies of the Bootlegger Cove Formation in southwest Anchorage, Alaska: Alaska Division of Geological and Geophysical Surveys Professional Report 84, 5 p., scale 1:15,840, 3 sheets.
- Updike, R.G., 1982, Engineering geologic facies of the Bootlegger Cove Formation, Anchorage, Alaska [abs.]: Geological Society of America Abstracts with Programs, v. 14, no. 7, p. 636.
- _____, 1983, Seismic liquefaction potential in the Anchorage area, south-central Alaska [abs.]: Symposium on the Engineering Geology of Liquefiable Deposits in the Western United States, Geological Society of America, Cordilleran and Rocky Mountain Section, Abstracts with Programs, v. 15, no. 5, p. 374.
- _____, 1985, Engineering geologic maps of the Government Hill area, Anchorage, Alaska: U.S. Geological Survey I-1610, scale 1:10,000, 1 sheet [in press].
- Updike, R.G., and Carpenter, B.A., 1985, Engineering geology of the Government Hill area, Anchorage, Alaska: U.S. Geological Survey Bulletin [in press].
- Updike, R.G., Cole, D.A., and Ulery, C.A., 1982, Shear moduli and damping ratios for the Bootlegger Cove Formation as determined by resonant-column testing, in Short notes on Alaskan geology - 1981: Alaska Division of Geological and Geophysical Surveys Professional Report 73, p. 7-12.
- Updike, R.G., and Ulery, C.A., 1985, Engineering geology of southwest Anchorage, Alaska: Alaska Division of Geological and Geophysical Surveys Professional Report 89 [in press].

APPENDIX

This appendix presents the tabulated data derived from digitization of the rectified CPT curves shown in figures 7 through 11. Soil-behavior types are based on computer tracking of friction ratio vs. cone resistance (figure 13). Undrained shear strengths, S_u , were computer calculated using the indicated empirical equations (see text for discussion).

DEPTH FT	CONE TSF	FRICTION TSF	RATIO	SOIL BEHAVIOR TYPES	SPT	SU=FS*1.10 (PSF)	SU=(C-T)/NC (PSF)
1.0	161.13	1.86	1.12	SAND TO SILTY SAND			
2.0	20.80	0.36	2.70	SENS. CLAYEY SI-SI CLAY		799.	2588.
3.0	3.49	0.40	11.01	CLAY		875.	419.
4.0	3.21	0.27	8.28	CLAY		593.	377.
5.0	3.33	0.26	7.53	CLAY		571.	387.
6.0	6.85	0.27	4.38	SILTY CLAY TO CLAY		596.	821.
7.0	61.78	0.34	0.90	SAND TO SILTY SAND			
8.0	39.36	0.51	1.43	SILTY SAND TO SANDY SILT			
9.0	106.91	0.55	0.73	SAND TO SILTY SAND			
10.0	19.39	0.50	2.71	SENS. CLAYEY SI-SI CLAY		1090.	2363.
11.0	27.97	1.50	5.32	SILTY CLAY TO CLAY		3306.	3430.
12.0	39.86	1.83	4.60	SILTY CLAY TO CLAY		4025.	4909.
13.0	40.62	2.38	5.72	SILTY CLAY TO CLAY		5231.	4998.
14.0	33.50	1.70	4.82	SILTY CLAY TO CLAY		3740.	4101.
15.0	31.67	1.52	4.96	SILTY CLAY TO CLAY		3343.	3857.
16.0	29.26	1.55	5.36	SILTY CLAY TO CLAY		3406.	3559.
17.0	37.36	1.55	4.36	SILTY CLAY TO CLAY		3410.	4566.
18.0	27.01	1.41	4.83	SILTY CLAY TO CLAY		3113.	3265.
19.0	29.93	1.20	4.12	SILTY CLAY TO CLAY		2644.	3624.
20.0	25.74	1.06	4.21	SILTY CLAY TO CLAY		2339.	3094.
21.0	28.36	1.36	4.45	SILTY CLAY TO CLAY		2999.	3416.
22.0	22.88	0.90	4.16	SILTY CLAY TO CLAY		1972.	2723.
23.0	22.47	1.04	4.50	SILTY CLAY TO CLAY		2289.	2666.
24.0	18.54	0.58	3.17	SILTY CLAY TO CLAY		1277.	2169.
25.0	32.31	1.64	4.24	SILTY CLAY TO CLAY		3503.	3884.
26.0	21.09	0.86	3.92	SILTY CLAY TO CLAY		1886.	2475.
27.0	18.46	0.72	3.98	SILTY CLAY TO CLAY		1593.	2141.
28.0	13.64	0.56	4.06	SILTY CLAY TO CLAY		1242.	1532.
29.0	19.62	0.66	3.69	SILTY CLAY TO CLAY		1448.	2273.
30.0	19.42	0.81	4.16	SILTY CLAY TO CLAY		1793.	2241.
31.0	16.63	0.64	3.82	SILTY CLAY TO CLAY		1412.	1886.
32.0	17.11	0.58	3.50	SILTY CLAY TO CLAY		1284.	1941.
33.0	14.48	0.46	3.28	SILTY CLAY TO CLAY		1015.	1606.
34.0	12.31	0.33	2.71	SENS. CLAYEY SI-SI CLAY		732.	1328.
35.0	14.77	0.60	4.09	SILTY CLAY TO CLAY		1309.	1629.
36.0	11.50	0.32	2.79	SENS. CLAYEY SI-SI CLAY		712.	1214.
37.0	11.33	0.29	2.52	SENS. CLAYEY SI-SI CLAY		628.	1187.
38.0	11.36	0.37	2.93	SILTY CLAY TO CLAY		808.	1184.
39.0	12.18	0.33	2.73	SENS. CLAYEY SI-SI CLAY		727.	1280.

EQ-1

DEPTH FT	CONE TSF	FRICTION TSF	RATIO	SOIL BEHAVIOR TYPES	SPT	SU=FS*1.10 (PSF)	SU=(C-T)/NC (PSF)
40.0	12.12	0.25	2.08	SENS. CLAYEY SI-SI CLAY		552.	1267.
41.0	11.78	0.28	2.18	SENS. CLAYEY SI-SI CLAY		609.	1218.
42.0	17.15	0.39	2.52	SENS. CLAYEY SI-SI CLAY		867.	1883.
43.0	11.81	0.25	2.17	SENS. CLAYEY SI-SI CLAY		587.	1209.
44.0	36.37	1.81	4.29	SILTY CLAY TO CLAY		3980.	4272.
45.0	16.57	0.15	0.92	SANDY SI TO CLAYEY SILT			
46.0	17.14	0.15	0.91	SANDY SI TO CLAYEY SILT			
47.0	16.13	0.15	0.70	SANDY SI TO CLAYEY SILT			
48.0	15.70	0.15	0.96	SANDY SI TO CLAYEY SILT			
49.0	15.20	0.16	1.01	SANDY SI TO CLAYEY SILT			
50.0	15.99	0.16	0.98	SANDY SI TO CLAYEY SILT			
51.0	17.50	0.18	1.02	SANDY SI TO CLAYEY SILT			
52.0	18.55	0.20	1.11	SANDY SI TO CLAYEY SILT			
53.0	21.50	0.26	1.23	SANDY SI TO CLAYEY SILT			
54.0	20.92	0.29	1.41	SANDY SI TO CLAYEY SILT			
55.0	22.88	0.61	3.00	SILTY CLAY		1343.	2517.
56.0	25.33	1.11	5.02	SILTY CLAY TO CLAY		2443.	2818.
57.0	19.08	0.94	4.91	SILTY CLAY TO CLAY		2074.	2030.
58.0	20.63	1.48	6.73	CLAY		3248.	2218.
59.0	20.12	1.29	6.41	CLAY		2838.	2147.
60.0	19.08	1.13	5.92	CLAY		2490.	2012.
61.0	19.78	1.45	5.60	CLAY		3201.	2093.
62.0	19.28	1.21	6.13	CLAY		2667.	2024.
63.0	20.17	1.07	5.54	CLAY		2355.	2130.
64.0	26.17	0.91	3.52	SILTY CLAY		2008.	2872.
65.0	30.49	1.13	3.57	SILTY CLAY		2495.	3407.
66.0	29.50	1.02	3.49	SILTY CLAY		2247.	3276.
67.0	24.54	0.84	3.35	SILTY CLAY		1842.	2650.
68.0	25.99	0.78	3.15	SILTY CLAY		1719.	2825.
69.0	51.64	1.34	3.16	SANDY CLAY TO SILTY CLAY		2958.	4821.
70.0	26.58	0.47	1.73	SANDY SI TO CLAYEY SILT			
71.0	25.98	0.63	2.36	SILTY CLAY		1396.	2805.
72.0	20.82	0.62	2.97	SILTY CLAY TO CLAY		1358.	2154.
73.0	30.29	0.93	3.28	SILTY CLAY		2048.	3332.
74.0	82.31	3.83	5.54	SILTY CLAY TO CLAY		8425.	9828.
75.0	60.68	4.27	6.21	CLAY		9398.	7118.
76.0	303.94	13.04	3.84	CLAYEY SA TO SANDY CLAY			

EQ-1

DEPTH FT	CONE TSF	FRICTION TSF	RATIO	SOIL BEHAVIOR TYPES	SPT	SU=F6*1.10 (PSF)	SU=(C-T)/NC (PSF)
1.0	483.28	4.76	1.05	SAND TO SILTY SAND			
2.0	140.33	0.91	1.03	SAND TO SILTY SAND			
3.0	8.09	0.51	5.88	CLAY		1113.	993.
4.0	8.16	0.63	7.42	CLAY		1379.	996.
5.0	8.23	0.53	6.31	CLAY		1168.	998.
6.0	8.29	0.47	5.60	CLAY		1024.	1001.
7.0	8.36	0.22	3.23	SILTY CLAY TO CLAY		474.	1003.
8.0	8.78	0.56	6.38	CLAY		1224.	1049.
9.0	7.89	0.28	3.81	SILTY CLAY TO CLAY		623.	931.
10.0	14.67	0.67	4.59	SILTY CLAY TO CLAY		1480.	1773.
11.0	15.96	0.73	3.99	SILTY CLAY TO CLAY		1603.	1928.
12.0	14.71	0.84	5.98	CLAY		1837.	1766.
13.0	17.91	0.97	5.49	CLAY		2136.	2158.
14.0	19.14	0.81	4.47	SILTY CLAY TO CLAY		1792.	2306.
15.0	21.25	0.86	4.22	SILTY CLAY TO CLAY		1896.	2564.
16.0	21.21	0.88	4.13	SILTY CLAY TO CLAY		1932.	2553.
17.0	14.89	0.84	5.16	SILTY CLAY TO CLAY		1856.	1757.
18.0	14.71	0.55	3.61	SILTY CLAY TO CLAY		1207.	1728.
19.0	14.63	0.65	4.13	SILTY CLAY TO CLAY		1437.	1712.
20.0	15.97	0.62	4.05	SILTY CLAY TO CLAY		1354.	1873.
21.0	15.22	0.45	3.28	SILTY CLAY TO CLAY		1000.	1772.
22.0	16.62	0.56	3.29	SILTY CLAY TO CLAY		1243.	1941.
23.0	18.96	0.74	4.01	SILTY CLAY TO CLAY		1621.	2228.
24.0	16.04	0.68	4.04	SILTY CLAY TO CLAY		1485.	1857.
25.0	15.34	0.61	4.03	SILTY CLAY TO CLAY		1338.	1763.
26.0	16.38	0.66	3.97	SILTY CLAY TO CLAY		1462.	1885.
27.0	16.75	0.58	3.49	SILTY CLAY TO CLAY		1275.	1926.
28.0	17.42	0.81	4.57	SILTY CLAY TO CLAY		1786.	2005.
29.0	16.43	0.66	4.14	SILTY CLAY TO CLAY		1462.	1875.
30.0	16.76	0.66	4.03	SILTY CLAY TO CLAY		1463.	1909.
31.0	15.14	0.51	3.42	SILTY CLAY TO CLAY		1118.	1700.
32.0	17.15	0.73	4.17	SILTY CLAY TO CLAY		1644.	1945.
33.0	15.66	0.50	3.44	SILTY CLAY TO CLAY		1090.	1752.
34.0	13.17	0.35	2.68	SENS. CLAYEY SI-SI CLAY		771.	1436.
35.0	11.91	0.49	3.49	SILTY CLAY TO CLAY		990.	1272.
36.0	11.96	0.32	2.71	SENS. CLAYEY SI-SI CLAY		703.	1271.
37.0	12.10	0.31	2.54	SENS. CLAYEY SI-SI CLAY		673.	1282.
38.0	12.15	0.33	2.69	SENS. CLAYEY SI-SI CLAY		722.	1283.
39.0	12.00	0.30	2.53	SENS. CLAYEY SI-SI CLAY		665.	1258.

EQ-2

DEPTH FT	CONE TSF	FRICTION TSF	RATIO	SOIL BEHAVIOR TYPES	SPT	SU=F6*1.10 (PSF)	SU=(C-T)/NC (PSF)
40.0	11.20	0.26	2.39	SENS. CLAYEY SI-SI CLAY		570.	1152.
41.0	11.31	0.24	2.12	SENS. CLAYEY SI-SI CLAY		520.	1159.
42.0	11.40	0.27	2.51	SENS. CLAYEY SI-SI CLAY		601.	1165.
43.0	27.73	0.90	4.83	SILTY CLAY TO CLAY		1978.	3199.
44.0	23.50	0.79	3.04	SILTY CLAY		1749.	2665.
45.0	13.21	0.20	2.65	SENS. CLAYEY SI-SI CLAY		434.	1371.
46.0	12.03	0.16	1.43	SENS. CLAYEY SI-SI CLAY		354.	1218.
47.0	12.57	0.16	1.62	SENS. CLAYEY SI-SI CLAY		359.	1279.
48.0	12.41	0.17	1.29	SENS. CLAYEY SI-SI CLAY		365.	1253.
49.0	12.06	0.14	1.21	SENS. CLAYEY SI-SI CLAY		308.	1203.
50.0	11.41	0.14	1.32	SENS. CLAYEY SI-SI CLAY		319.	1115.
51.0	11.68	0.16	1.34	SENS. CLAYEY SI-SI CLAY		343.	1143.
52.0	11.97	0.16	1.33	SENS. CLAYEY SI-SI CLAY		346.	1172.
53.0	12.29	0.14	1.18	SENS. CLAYEY SI-SI CLAY		304.	1207.
54.0	11.59	0.13	1.19	SENS. CLAYEY SI-SI CLAY		297.	1113.
55.0	13.59	0.16	1.22	SANDY SI TO CLAYEY SILT			
56.0	15.47	0.27	1.76	SENS. CLAYEY SI-SI CLAY		603.	1585.
57.0	16.31	0.31	1.89	SENS. CLAYEY SI-SI CLAY		677.	1685.
58.0	16.41	0.32	1.91	SENS. CLAYEY SI-SI CLAY		695.	1690.
59.0	17.34	0.33	1.92	SENS. CLAYEY SI-SI CLAY		734.	1800.
60.0	17.46	0.32	1.88	SENS. CLAYEY SI-SI CLAY		710.	1809.
61.0	17.59	0.33	1.88	SENS. CLAYEY SI-SI CLAY		715.	1819.
62.0	18.45	0.37	1.93	SENS. CLAYEY SI-SI CLAY		822.	1920.
63.0	21.27	0.18	1.72	SANDY SI TO CLAYEY SILT			
64.0	23.25	0.51	2.44	SILTY CLAY		1116.	2507.
65.0	25.33	0.75	3.00	SILTY CLAY		1644.	2761.
66.0	22.98	1.18	5.06	SILTY CLAY TO CLAY		2590.	2462.
67.0	22.66	1.03	4.53	SILTY CLAY TO CLAY		2271.	2415.
68.0	21.34	0.92	4.24	SILTY CLAY TO CLAY		2014.	2244.
69.0	19.78	0.73	3.98	SILTY CLAY TO CLAY		1602.	1918.
70.0	19.36	0.71	3.74	SILTY CLAY TO CLAY		1572.	1984.
71.0	19.36	0.59	3.09	SILTY CLAY TO CLAY		1294.	1978.
72.0	18.29	0.47	2.82	SENS. CLAYEY SI-SI CLAY		1031.	1838.
73.0	21.41	0.48	2.20	SILTY CLAY		1048.	2222.
74.0	23.92	0.51	2.21	SILTY CLAY		1122.	2529.
75.0	23.08	0.54	2.37	SILTY CLAY		1195.	2418.
76.0	23.79	0.67	2.63	SILTY CLAY		1475.	2750.
77.0	25.03	0.66	2.64	SILTY CLAY		1458.	2650.
78.0	29.57	0.81	2.80	SILTY CLAY		1790.	3210.
79.0	26.39	0.91	3.23	SILTY CLAY		1997.	2807.
80.0	25.76	0.89	3.22	SILTY CLAY		1955.	2747.

EQ-2

DEPTH FT	CONE TSF	FRICTION TSF	RATIO	SOIL BEHAVIOR TYPES	SPT	SU=FS*1.10 (PSF)	SU=(C-T)/NC (PSF)
81.0	29.50	0.93	2.91	SILTY CLAY		2041.	3183.
82.0	60.54	1.43	2.79	SANDY CLAY TO SILTY CLAY		3142.	5647.
83.0	230.87	4.89	2.33	SILTY SA TO CLAYEY SAND			
84.0	200.78	13.00	6.80	CLAY		28606.	24575.
85.0	320.49	10.00	3.26	CLAYEY SA TO SANDY CLAY			
86.0	255.35	9.21	4.07	SANDY CLAY TO SILTY CLAY		20257.	26156.
87.0	107.70	11.85	8.68	CLAY		26059.	12920.
88.0	80.59	4.73	5.12	SILTY CLAY TO CLAY		10406.	9537.
89.0	213.37	4.58	2.37	SILTY SA TO CLAYEY SAND			
90.0	161.85	4.62	3.02	CLAYEY SA TO SANDY CLAY			
91.0	34.65	1.91	2.76	SILTY CLAY		4208.	3764.
92.0	183.21	8.95	4.60	SANDY CLAY TO SILTY CLAY		19699.	17862.
93.0	59.76	0.89	2.05	SILTY SAND TO SANDY SILT			

EQ-2

DEPTH FT	CONE TSF	FRICTION TSF	RATIO	SOIL BEHAVIOR TYPES	SPT	SU=FS*1.10 (PSF)	SU=(C-T)/NC (PSF)
1.0	103.75	0.46	0.60	SAND TO SILTY SAND			
2.0	6.74	0.81	11.08	CLAY		1782.	830.
3.0	2.63	0.49	17.93	CLAY		1088.	355.
4.0	2.34	0.39	15.91	CLAY		851.	308.
5.0	11.24	0.26	2.40	SENS. CLAYEY SI-SI CLAY		565.	1375.
6.0	22.95	0.44	2.04	SANDY SI TO CLAYEY SILT			
7.0	7.63	0.20	2.22	SENS. CLAYEY SI-SI CLAY		430.	917.
8.0	10.26	0.32	3.02	SILTY CLAY TO CLAY		713.	1234.
9.0	21.73	0.53	3.82	SILTY CLAY		1156.	2662.
10.0	20.20	0.57	3.20	SILTY CLAY TO CLAY		1262.	2464.
11.0	18.96	0.75	3.94	SILTY CLAY TO CLAY		1658.	2303.
12.0	15.21	0.74	3.76	SILTY CLAY TO CLAY		1622.	1828.
13.0	18.78	0.50	2.80	SENS. CLAYEY SI-SI CLAY		1095.	2268.
14.0	15.92	0.50	3.15	SILTY CLAY TO CLAY		1104.	1904.
15.0	20.18	0.66	3.37	SILTY CLAY TO CLAY		1448.	2430.
16.0	12.05	0.41	3.15	SILTY CLAY TO CLAY		913.	1407.
17.0	17.20	0.65	3.43	SILTY CLAY TO CLAY		1437.	2045.
18.0	32.69	0.72	2.35	SANDY SI TO CLAYEY SILT			
19.0	13.66	0.38	2.59	SENS. CLAYEY SI-SI CLAY		827.	1590.
20.0	14.87	0.54	3.47	SILTY CLAY TO CLAY		1192.	1736.
21.0	21.38	0.55	2.77	SILTY CLAY		1204.	2543.
22.0	13.10	0.33	2.74	SENS. CLAYEY SI-SI CLAY		722.	1501.
23.0	18.65	0.65	3.93	SILTY CLAY TO CLAY		1432.	2189.
24.0	13.29	0.43	3.33	SILTY CLAY TO CLAY		938.	1512.
25.0	13.81	0.44	3.33	SILTY CLAY TO CLAY		974.	1572.
26.0	11.93	0.42	3.58	SILTY CLAY TO CLAY		927.	1330.
27.0	12.47	0.46	3.67	SILTY CLAY TO CLAY		1016.	1392.
28.0	13.49	0.55	3.91	SILTY CLAY TO CLAY		1215.	1513.
29.0	14.98	0.37	2.65	SENS. CLAYEY SI-SI CLAY		816.	1692.
30.0	12.44	0.42	3.49	SILTY CLAY TO CLAY		934.	1369.
31.0	16.53	0.47	3.03	SILTY CLAY TO CLAY		1024.	1874.
32.0	9.22	0.33	3.52	SILTY CLAY TO CLAY		726.	954.
33.0	9.66	0.21	2.19	SENS. CLAYEY SI-SI CLAY		467.	1003.
34.0	9.40	0.22	2.40	SENS. CLAYEY SI-SI CLAY		494.	964.
35.0	9.05	0.15	1.63	SENS. CLAYEY SI-SI CLAY		330.	914.
36.0	9.30	0.16	1.77	SENS. CLAYEY SI-SI CLAY		356.	939.
37.0	8.03	0.34	3.68	SILTY CLAY TO CLAY		747.	774.
38.0	10.51	0.51	3.53	SILTY CLAY TO CLAY		1128.	1077.
39.0	17.40	1.42	6.74	CLAY		3114.	1933.

EQ-3

DEPTH FT	CONE TSF	FRICTION TSF	RATIO	SOIL BEHAVIOR TYPES	SPT	SU=FS*1.10 (PSF)	SU=(C-T)/NC (PSF)
40.0	26.63	2.03	6.91	CLAY		4474.	3080.
41.0	10.38	0.24	2.41	SENS. CLAYEY SI-SI CLAY		536.	1043.
42.0	9.87	0.23	2.45	SENS. CLAYEY SI-SI CLAY		506.	973.
43.0	9.65	0.27	2.84	SENS. CLAYEY SI-SI CLAY		594.	939.
44.0	13.12	0.55	5.41	CLAY		1216.	1367.
45.0	11.03	0.61	5.87	CLAY		1338.	1099.
45.0	10.29	0.32	3.01	SILTY CLAY TO CLAY		706.	1001.
47.0	8.30	0.20	2.41	SENS. CLAYEY SI-SI CLAY		435.	746.
48.0	9.51	0.23	2.82	SENS. CLAYEY SI-SI CLAY		514.	890.
49.0	7.19	0.18	2.47	SENS. CLAYEY SI-SI CLAY		395.	594.
50.0	9.58	0.26	2.76	SENS. CLAYEY SI-SI CLAY		576.	887.
51.0	8.48	0.22	2.61	SENS. CLAYEY SI-SI CLAY		490.	743.
52.0	8.79	0.23	2.40	SENS. CLAYEY SI-SI CLAY		510.	776.
53.0	9.02	0.21	2.39	SENS. CLAYEY SI-SI CLAY		472.	797.
54.0	9.36	0.21	2.24	SENS. CLAYEY SI-SI CLAY		457.	834.
55.0	9.52	0.22	2.34	SENS. CLAYEY SI-SI CLAY		487.	848.
56.0	9.24	0.19	2.17	SENS. CLAYEY SI-SI CLAY		417.	807.
57.0	10.07	0.23	2.72	SENS. CLAYEY SI-SI CLAY		515.	904.
58.0	12.89	0.37	3.83	SILTY CLAY TO CLAY		1254.	1250.
59.0	12.35	0.31	2.31	SENS. CLAYEY SI-SI CLAY		675.	1176.
60.0	12.43	0.23	1.87	SENS. CLAYEY SI-SI CLAY		508.	1180.
61.0	11.98	0.20	1.74	SENS. CLAYEY SI-SI CLAY		443.	1118.
62.0	11.75	0.25	2.10	SENS. CLAYEY SI-SI CLAY		544.	1083.
63.0	13.79	0.26	1.95	SENS. CLAYEY SI-SI CLAY		576.	1332.
64.0	13.90	0.27	2.02	SENS. CLAYEY SI-SI CLAY		599.	1339.
65.0	37.69	1.20	4.34	SILTY CLAY TO CLAY		2642.	4306.
65.0	14.09	0.29	2.12	SENS. CLAYEY SI-SI CLAY		634.	1350.
67.0	15.24	0.33	2.16	SENS. CLAYEY SI-SI CLAY		721.	1488.
68.0	15.69	0.36	2.28	SENS. CLAYEY SI-SI CLAY		797.	1537.
69.0	16.04	0.37	2.31	SENS. CLAYEY SI-SI CLAY		815.	1575.
70.0	18.45	0.46	2.52	SENS. CLAYEY SI-SI CLAY		1005.	1871.
71.0	22.09	0.57	2.73	SILTY CLAY		1247.	2320.
72.0	18.76	0.46	2.22	SENS. CLAYEY SI-SI CLAY		1010.	1897.
73.0	16.47	0.40	2.39	SENS. CLAYEY SI-SI CLAY		871.	1604.
74.0	15.73	0.37	2.25	SENS. CLAYEY SI-SI CLAY		806.	1505.
75.0	15.49	0.35	2.21	SENS. CLAYEY SI-SI CLAY		762.	1469.
75.0	15.37	0.32	2.05	SENS. CLAYEY SI-SI CLAY		701.	1447.
77.0	15.36	0.33	2.13	SENS. CLAYEY SI-SI CLAY		716.	1441.
78.0	15.32	0.30	1.98	SENS. CLAYEY SI-SI CLAY		664.	1429.
79.0	15.40	0.28	1.82	SENS. CLAYEY SI-SI CLAY		618.	1432.
80.0	15.62	0.31	1.86	SENS. CLAYEY SI-SI CLAY		683.	1454.

EQ-3

DEPTH FT	CONE TSF	FRICTION TSF	RATIO	SOIL BEHAVIOR TYPES	SPT	SU=F8*1.10 (PSF)	SU=(C-T)/NC (PSF)
81.0	16.35	0.32	1.87	SENS. CLAYEY SI-SI CLAY		707.	1540.
82.0	15.72	0.30	1.92	SENS. CLAYEY SI-SI CLAY		658.	1454.
83.0	17.04	0.35	2.06	SENS. CLAYEY SI-SI CLAY		764.	1613.
84.0	17.82	0.37	2.05	SENS. CLAYEY SI-SI CLAY		814.	1705.
85.0	17.67	0.37	2.04	SENS. CLAYEY SI-SI CLAY		805.	1679.
86.0	17.61	0.35	1.99	SENS. CLAYEY SI-SI CLAY		777.	1666.
87.0	16.89	0.33	1.93	SENS. CLAYEY SI-SI CLAY		729.	1569.
88.0	16.64	0.31	1.88	SENS. CLAYEY SI-SI CLAY		680.	1531.
89.0	16.84	0.33	2.03	SENS. CLAYEY SI-SI CLAY		764.	1551.
90.0	17.38	0.33	1.92	SENS. CLAYEY SI-SI CLAY		718.	1612.
91.0	17.48	0.36	2.05	SENS. CLAYEY SI-SI CLAY		785.	1618.
92.0	17.64	0.35	1.97	SENS. CLAYEY SI-SI CLAY		772.	1632.
93.0	20.88	0.40	2.15	SENS. CLAYEY SI-SI CLAY		885.	2030.
94.0	17.90	0.49	2.73	SENS. CLAYEY SI-SI CLAY		1073.	1452.
95.0	18.25	0.41	2.26	SENS. CLAYEY SI-SI CLAY		895.	1689.
96.0	17.88	0.38	1.98	SENS. CLAYEY SI-SI CLAY		828.	1636.
97.0	19.47	0.40	2.07	SENS. CLAYEY SI-SI CLAY		874.	1829.
98.0	18.88	0.33	1.78	SANDY SI TO CLAYEY SILT			
99.0	18.81	0.57	3.02	SILTY CLAY TO CLAY		1247.	1734.
100.0	17.08	0.37	2.26	SENS. CLAYEY SI-SI CLAY		820.	1512.
101.0	41.58	1.47	3.50	SANDY CLAY TO SILTY CLAY		3229.	3654.
102.0	56.06	4.04	5.29	SILTY CLAY TO CLAY		8891.	6371.
103.0	162.57	5.51	3.71	CLAYEY SA TO SANDY CLAY			
104.0	113.00	4.98	4.15	SANDY CLAY TO SILTY CLAY		10954.	10781.
105.0	198.44	5.77	3.08	CLAYEY SA TO SANDY CLAY			
106.0	45.55	1.75	3.11	SANDY CLAY TO SILTY CLAY		3850.	4026.
107.0	85.00	3.49	3.62	SANDY CLAY TO SILTY CLAY		7672.	7966.
108.0	191.28	4.01	2.97	CLAYEY SA TO SANDY CLAY			
109.0	147.47	3.16	2.37	SILTY SA TO CLAYEY SAND			
110.0	29.34	0.55	2.16	SANDY SI TO CLAYEY SILT			
111.0	151.82	5.10	3.29	CLAYEY SA TO SANDY CLAY			
112.0	28.63	1.14	4.05	SILTY CLAY TO CLAY		2511.	2880.
113.0	277.23	8.70	3.21	CLAYEY SA TO SANDY CLAY			
114.0	182.65	5.90	3.00	CLAYEY SA TO SANDY CLAY			
115.0	115.89	2.47	2.67	CLAYEY SA TO SANDY CLAY			
116.0	85.98	2.31	2.82	CLAYEY SA TO SANDY CLAY			
117.0	31.72	0.49	2.09	SANDY SI TO CLAYEY SILT			
118.0	342.52	11.16	3.29	CLAYEY SA TO SANDY CLAY			
119.0	216.30	6.64	3.09	CLAYEY SA TO SANDY CLAY			
120.0	90.31	2.85	2.96	CLAYEY SA TO SANDY CLAY			
121.0	67.36	2.43	3.18	SANDY CLAY TO SILTY CLAY		5347.	6132.

EQ-3

DEPTH FT	CONE TSF	FRICTION TSF	RATIO	SOIL BEHAVIOR TYPES	SPT	SU=FS*1.10 (PSF)	SU=(C-T)/NC (PSF)
1.0	105.34	0.46	1.80	SILTY SAND TO SANDY SILT			
2.0	15.66	0.51	7.43	CLAY		1114.	1946.
3.0	2.38	0.47	19.56	CLAY		1044.	320.
4.0	2.60	0.46	19.39	CLAY		1023.	344.
5.0	6.96	0.74	14.33	CLAY		1627.	960.
6.0	6.11	0.47	8.02	CLAY		1041.	727.
7.0	5.15	0.43	8.98	CLAY		954.	602.
8.0	10.25	0.91	9.31	CLAY		1994.	1233.
9.0	15.86	1.03	6.51	CLAY		2256.	1928.
10.0	18.24	1.18	6.97	CLAY		2606.	2219.
11.0	18.69	1.39	7.72	CLAY		3062.	2269.
12.0	22.17	1.65	7.33	CLAY		3628.	2698.
13.0	22.18	1.35	6.04	CLAY		2968.	2693.
14.0	17.70	0.99	5.54	CLAY		2168.	2127.
15.0	19.76	1.05	5.51	CLAY		2308.	2378.
16.0	18.10	1.15	6.31	CLAY		2538.	2164.
17.0	19.68	0.84	5.54	CLAY		1851.	1856.
18.0	22.17	1.30	6.09	CLAY		2857.	2660.
19.0	18.63	0.95	5.04	SILTY CLAY TO CLAY		2093.	2212.
20.0	16.62	0.83	5.05	SILTY CLAY TO CLAY		1833.	1954.
21.0	15.34	0.82	5.38	CLAY		1799.	1788.
22.0	18.72	1.11	5.62	CLAY		2436.	2204.
23.0	18.95	0.94	5.24	SILTY CLAY TO CLAY		2077.	2226.
24.0	17.15	1.12	5.83	CLAY		2463.	1996.
25.0	18.15	1.01	5.58	CLAY		2228.	2114.
26.0	16.59	0.79	4.88	SILTY CLAY TO CLAY		1737.	1913.
27.0	12.87	0.96	7.99	CLAY		2107.	1441.
28.0	34.27	1.19	5.18	SILTY CLAY TO CLAY		2620.	4111.
29.0	11.85	0.92	7.00	CLAY		2016.	1302.
30.0	13.13	0.58	4.59	SILTY CLAY TO CLAY		1281.	1455.
31.0	11.13	0.58	5.04	SILTY CLAY TO CLAY		1269.	1199.
32.0	9.61	0.49	5.17	CLAY		1074.	1003.
33.0	9.90	0.50	5.00	SILTY CLAY TO CLAY		1089.	1033.
34.0	9.98	0.49	4.96	SILTY CLAY TO CLAY		1073.	1037.
35.0	9.87	0.46	4.71	SILTY CLAY TO CLAY		1020.	1016.
36.0	11.99	0.81	6.57	CLAY		1771.	1275.
37.0	9.92	0.50	5.11	CLAY		1102.	1010.
38.0	9.08	2.26	9.41	CLAY		4971.	3400.
39.0	11.29	0.44	3.68	SILTY CLAY TO CLAY		958.	1169.

EQ-4

DEPTH FT	CONE TSF	FRICTION TSF	RATIO	SOIL BEHAVIOR TYPES	SPT	SU=FS*1.10 (PSF)	SU=(C-T)/NC (PSF)
40.0	16.72	0.60	4.01	SILTY CLAY TO CLAY		1314.	1841.
41.0	11.90	0.40	3.51	SILTY CLAY TO CLAY		888.	1233.
42.0	11.23	0.39	3.42	SILTY CLAY TO CLAY		867.	1143.
43.0	10.38	0.38	3.55	SILTY CLAY TO CLAY		832.	1031.
44.0	10.12	0.39	3.69	SILTY CLAY TO CLAY		848.	992.
45.0	10.57	0.32	3.12	SILTY CLAY TO CLAY		714.	1054.
46.0	39.20	0.64	4.14	SILTY CLAY TO CLAY		1417.	4614.
47.0	11.17	0.37	3.26	SILTY CLAY TO CLAY		805.	1104.
48.0	12.13	0.37	3.38	SILTY CLAY TO CLAY		824.	1218.
49.0	12.80	0.43	3.27	SILTY CLAY TO CLAY		943.	1296.
50.0	15.63	0.50	3.43	SILTY CLAY TO CLAY		1110.	1643.
51.0	16.81	0.66	3.77	SILTY CLAY TO CLAY		1451.	1785.
52.0	18.90	0.70	3.66	SILTY CLAY TO CLAY		1529.	2039.
53.0	16.50	0.58	3.57	SILTY CLAY TO CLAY		1273.	1733.
54.0	16.99	0.65	4.02	SILTY CLAY TO CLAY		1431.	1788.
55.0	17.61	1.69	6.10	CLAY		3714.	1859.
56.0	16.98	0.60	3.38	SILTY CLAY TO CLAY		1328.	1774.
57.0	18.79	0.68	3.62	SILTY CLAY TO CLAY		1504.	1994.
58.0	19.94	0.71	3.61	SILTY CLAY TO CLAY		1556.	2132.
59.0	19.77	0.70	3.55	SILTY CLAY TO CLAY		1547.	2104.
60.0	16.98	0.63	3.61	SILTY CLAY TO CLAY		1386.	1749.
61.0	15.17	0.63	4.27	SILTY CLAY TO CLAY		1382.	1517.
62.0	19.28	0.65	3.43	SILTY CLAY TO CLAY		1436.	2024.
63.0	16.68	0.54	3.28	SILTY CLAY TO CLAY		1198.	1693.
64.0	13.60	0.63	4.51	SILTY CLAY TO CLAY		1396.	1301.
65.0	15.67	0.55	3.61	SILTY CLAY TO CLAY		1214.	1554.
66.0	14.75	0.59	3.91	SILTY CLAY TO CLAY		1298.	1433.
67.0	13.41	0.60	4.26	SILTY CLAY TO CLAY		1312.	1259.
68.0	11.69	0.58	4.97	SILTY CLAY TO CLAY		1265.	1037.
69.0	14.33	0.71	4.95	SILTY CLAY TO CLAY		1554.	1362.
70.0	13.97	0.68	5.19	SILTY CLAY TO CLAY		1493.	1310.
71.0	19.21	1.61	7.76	CLAY		3538.	1959.
72.0	16.14	1.32	7.92	CLAY		2902.	1569.
73.0	68.76	4.28	5.07	SILTY CLAY TO CLAY		9424.	8141.
74.0	34.74	2.56	6.92	CLAY		5622.	3882.
75.0	221.54	6.73	3.33	CLAYEY SA TO SANDY CLAY			
76.0	97.32	3.91	3.88	SANDY CLAY TO SILTY CLAY		8597.	9354.
77.0	180.71	6.04	3.11	CLAYEY SA TO SANDY CLAY			
78.0	25.62	0.32	1.37	SANDY SI TO CLAYEY SILT			
79.0	21.99	0.62	3.50	SILTY CLAY		1358.	2257.
80.0	134.26	4.52	3.41	CLAYEY SA TO SANDY CLAY			

EQ-4

DEPTH FT	CONE TSF	FRICTION TSF	RATIO	SOIL BEHAVIOR TYPES	SPT	SU=FS*1.10 (PSF)	SU=(C-T)/NC (PSF)
81.0	132.28	3.94	3.54	CLAYEY SA TO SANDY CLAY			
82.0	48.63	1.67	4.00	SANDY CLAY TO SILTY CLAY		3674.	4454.
83.0	95.89	4.06	5.39	SILTY CLAY TO CLAY		8929.	11469.
84.0	153.77	5.50	4.65	SANDY CLAY TO SILTY CLAY		12105.	14959.
85.0	197.67	8.10	4.53	SANDY CLAY TO SILTY CLAY		17815.	19343.
86.0	177.30	10.75	5.51	SILTY CLAY TO CLAY		23653.	21626.
EQ-4							

DEPTH FT	CONE TSF	FRICTION TSF	RATIO	SOIL BEHAVIOR TYPES	SPT	SU=FS*1.10 (PSF)	SU=(C-T)/NC (PSF)
1.0	0.04	0.00	0.00				
2.0	0.07	0.00	0.00				
3.0	0.53	0.14	27.09	CLAY		315.	55.
4.0	1.38	0.31	21.81	CLAY		671.	170.
5.0	2.23	0.42	16.63	CLAY		922.	285.
6.0	4.45	0.28	6.68	CLAY		613.	520.
7.0	5.09	0.32	6.52	CLAY		698.	594.
8.0	7.05	0.49	6.91	CLAY		1070.	833.
9.0	12.70	0.79	6.43	CLAY		1744.	1533.
10.0	22.99	1.18	5.47	SILTY CLAY TO CLAY		2589.	2813.
11.0	21.00	0.97	4.55	SILTY CLAY TO CLAY		2139.	2558.
12.0	22.36	1.38	5.70	CLAY		3033.	2722.
13.0	18.17	1.13	6.03	CLAY		2489.	2192.
14.0	14.95	0.83	5.46	CLAY		1830.	1783.
15.0	17.19	0.79	4.75	SILTY CLAY TO CLAY		1744.	2057.
16.0	18.22	0.90	5.02	SILTY CLAY TO CLAY		1983.	2179.
17.0	17.48	0.73	4.34	SILTY CLAY TO CLAY		1606.	2080.
18.0	18.57	0.66	3.53	SILTY CLAY TO CLAY		1458.	2210.
19.0	21.17	1.02	4.48	SILTY CLAY TO CLAY		2239.	2529.
20.0	17.93	0.78	4.33	SILTY CLAY TO CLAY		1716.	2118.
21.0	15.79	0.65	4.17	SILTY CLAY TO CLAY		1425.	1844.
22.0	15.90	0.74	4.71	SILTY CLAY TO CLAY		1628.	1851.
23.0	16.93	0.69	4.15	SILTY CLAY TO CLAY		1525.	1974.
24.0	18.13	0.71	3.95	SILTY CLAY TO CLAY		1564.	2118.
25.0	19.53	0.86	4.47	SILTY CLAY TO CLAY		1891.	2286.
26.0	18.47	0.75	4.02	SILTY CLAY TO CLAY		1651.	2148.
27.0	25.15	1.24	4.48	SILTY CLAY TO CLAY		2730.	2976.
28.0	13.27	0.53	4.00	SILTY CLAY TO CLAY		1169.	1486.
29.0	12.38	0.48	3.89	SILTY CLAY TO CLAY		1059.	1367.
30.0	13.46	0.48	3.54	SILTY CLAY TO CLAY		1050.	1497.
31.0	12.48	0.50	4.00	SILTY CLAY TO CLAY		1089.	1368.
32.0	11.25	0.50	4.41	SILTY CLAY TO CLAY		1094.	1208.
33.0	10.40	0.48	4.54	SILTY CLAY TO CLAY		1056.	1095.
34.0	10.86	0.53	4.72	SILTY CLAY TO CLAY		1171.	1146.
35.0	12.64	0.51	4.35	SILTY CLAY TO CLAY		1115.	1363.
36.0	10.56	0.45	4.18	SILTY CLAY TO CLAY		986.	1096.
37.0	14.75	0.45	3.31	SILTY CLAY TO CLAY		991.	1615.
38.0	10.44	0.43	5.35	CLAY		952.	1069.
39.0	13.25	0.83	4.94	SILTY CLAY TO CLAY		1823.	1414.

EQ-5

DEPTH FT	CONE TSF	FRICTION TSF	RATIO	SOIL BEHAVIOR TYPES	SPT	SU=FB*1.10 (PSF)	SU=(C-T)/NC (PSF)
40.0	10.74	0.43	3.95	SILTY CLAY TO CLAY		945.	1094.
41.0	11.22	0.39	3.78	SILTY CLAY TO CLAY		864.	1147.
42.0	11.02	0.42	3.80	SILTY CLAY TO CLAY		928.	1116.
43.0	10.18	0.38	3.68	SILTY CLAY TO CLAY		837.	1005.
44.0	10.22	0.39	3.73	SILTY CLAY TO CLAY		869.	1004.
45.0	10.89	0.53	4.14	SILTY CLAY TO CLAY		1171.	1077.
46.0	13.97	0.48	3.95	SILTY CLAY TO CLAY		1048.	1460.
47.0	13.61	0.45	3.39	SILTY CLAY TO CLAY		999.	1409.
48.0	13.91	0.47	3.47	SILTY CLAY TO CLAY		1043.	1440.
49.0	15.01	0.51	3.39	SILTY CLAY TO CLAY		1113.	1572.
50.0	16.41	0.57	3.52	SILTY CLAY TO CLAY		1258.	1740.
51.0	17.04	0.52	3.14	SILTY CLAY TO CLAY		1143.	1813.
52.0	18.58	0.69	3.67	SILTY CLAY TO CLAY		1517.	1999.
53.0	18.06	0.16	2.46	SENS. CLAYEY SI-SI CLAY		342.	1927.
54.0	20.28	0.63	3.18	SILTY CLAY TO CLAY		1382.	2198.
55.0	21.05	0.77	3.54	SILTY CLAY TO CLAY		1702.	2289.
56.0	20.34	0.73	3.51	SILTY CLAY TO CLAY		1611.	2194.
57.0	21.64	0.77	3.41	SILTY CLAY		1693.	2350.
58.0	21.36	0.68	3.27	SILTY CLAY TO CLAY		1497.	2309.
59.0	19.83	0.71	3.49	SILTY CLAY TO CLAY		1561.	2112.
60.0	21.63	0.72	3.39	SILTY CLAY		1590.	2330.
61.0	20.88	0.71	3.42	SILTY CLAY TO CLAY		1572.	2230.
62.0	21.68	0.71	3.32	SILTY CLAY		1569.	2324.
63.0	18.68	0.57	3.22	SILTY CLAY TO CLAY		1264.	1942.
64.0	16.02	0.56	3.46	SILTY CLAY TO CLAY		1225.	1604.
65.0	18.38	0.63	3.39	SILTY CLAY TO CLAY		1375.	1892.
66.0	14.41	0.51	3.57	SILTY CLAY TO CLAY		1129.	1390.
67.0	12.09	0.52	4.33	SILTY CLAY TO CLAY		1143.	1095.
68.0	14.82	0.52	3.74	SILTY CLAY TO CLAY		1140.	1429.
69.0	17.52	0.63	3.74	SILTY CLAY TO CLAY		1393.	1760.
70.0	33.64	0.63	2.65	SILTY CLAY		1390.	3769.
71.0	45.70	1.49	3.59	SANDY CLAY TO SILTY CLAY		3283.	4217.
72.0	38.97	2.02	4.03	SILTY CLAY TO CLAY		4438.	4423.
73.0	142.06	3.54	3.07	CLAYEY SA TO SANDY CLAY			
74.0	110.11	2.03	1.75	SILTY SAND TO SANDY SILT			
75.0	29.27	1.82	5.63	SILTY CLAY TO CLAY		4003.	3192.
76.0	51.49	1.17	1.55	SILTY SAND TO SANDY SILT			
77.0	123.68	1.56	1.61	SAND TO SILTY SAND			
78.0	74.25	0.93	2.08	SILTY SAND TO SANDY SILT			
79.0	172.80	2.38	1.61	SAND TO SILTY SAND			

EQ-5